International Atomic Energy Agency

INDC(CCP)-304/L

INDC INTERNATIONAL NUCLEAR DATA COMMITTEE

TRANSLATION OF SELECTED PAPERS PUBLISHED IN NUCLEAR CONSTANTS 1, 1987

(Original Report in Russian was distributed as INDC(CCP)-276/G)

Translated by the IAEA

September 1989

IAEA NUCLEAR DATA SECTION, WAGRAMERSTRASSE 5, A-1400 VIENNA

INDC(CCP)-304/L

TRANSLATION OF SELECTED PAPERS
PUBLISHED IN NUCLEAR CONSTANTS 1, 1987

(Original Report in Russian was distributed
as INDC(CCP)-276/G)

Translated by the IAEA

September 1989

Reproduced by the IAEA in Austria
October 1989

89-04724

Contents

THE LIBRARY OF RECOMMENDED EVALUATED NEUTRON CROSS-SECTIONS FOR THE MOST IMPORTANT NUCLEAR FISSION PRODUCTS

A.V. Ignatyuk, I.V. Kravchenko, G.N. Manturov

At the present time great importance is attached to the problem of developing reliable evaluated neutron cross-sections for the nuclear fission products which determine the poisoning of a fast reactor core and the activity of reprocessed nuclear fuel. A large number of such evaluations exist, the most comprehensive compilations being CNEN [1], RCN-II [2], JENDL-I [3] and ENDF/B-V [4].

Evaluated neutron radiative capture cross-sections are of great interest in solving practical problems. For many fission products, the capture cross-section evaluations in the above compilations show significant discrepancies, these being particularly evident from new experimental data obtained since the time the evaluations were performed. In order to eliminate these discrepancies, the Nuclear Data Centre of the USSR State Committee on the Utilization of Atomic Energy has analysed all existing experimental data on resonance and fast neutron radiative capture cross-sections. As a result, new evaluations of capture cross-sections were obtained for the isotopes ^{99}Tc, ^{101,102,104}Ru, ^{103}Rh, ^{105,107}Pd, ^{109}Ag, ^{129}I, ^{131}Xe, ^{143,145}Nd, ^{147}Pm, ^{147,149,151}Sm. It was demonstrated that new evaluations were not required for the isotopes ^{95,97,98,100}Mo, ^{133}Cs, ^{141}Pr, ^{151,153}Eu, as the recommendations of the JENDL-I or ENDF/B-V libraries are optimal. Following this review, a library of recommended evaluated neutron data was compiled for the 27 most important fission products. This paper briefly describes the evaluations included in the library and analyses the errors associated with them.

Table 1 contains a list of the nuclear fission products which contribute most to neutron absorption in fast reactor cores. The last three columns of Table 1 show existing experimental data on thermal neutron capture cross-sections [5], on capture resonance integrals and average neutron capture

Table 1. Characteristics of the most important fission products accumulating in fast reactor cores

Isotope	Ranking of fission product [1]	Contribution to absorption, %	Thermal neutron capture cross-section, b	Capture resonance integral, b	Average capture cross-section for the CFRMF assembly, b
^{105}Pd	I	9,9	20±3*	98*	-
^{99}To	2	8,6	20±I	340±20	0,267±40
^{101}Ru	3	7,7	3,4±0,9	I00±20	-
^{107}Pd	4	6,2	I,8±0,2*	86,6*	-
^{103}Rh	5	5,5	I45±2	II00±50	0,376±0,090
^{133}Cs	6	4,9	29,0±I,5	437± 26	0,276±0,0I8
^{147}Pm	7	3,5	I68,4±3,5	2064±I00	0,64I±0,085
^{149}Sm	8	3,4	3390*	40I40±600	-
^{145}Nd	9	3,4	42±2	240± 35	-
^{102}Ru	I0	3,3	I,2I±0,07	4,2±0,I	0,089±0,006
^{135}Cs	II	3,0	8,7±0,5	62±2	-
^{97}Mo	I2	2,9	2,I±0,5	I4±3	-
^{109}Ag	I3	2,7	9I±I	I400±48	0,507±0,50
^{106}Ru	I4	2,3	0,I46±0,045	-	-
^{143}Nd	I5	2,3	325±I0	528±30	-
^{131}Xe	I6	I,9	85±I0	900±I00	-
^{151}Sm	I7	I,9	I5200±300	3520±I80*	-
^{95}Mo	I8	I,5	I4,0±0,5	I09±5	-
^{104}Ru	I9	I,3	0,32±0,02	4,3±0,I	0,083±0,005
^{153}Eu	20	I,3	3I2±7	I420±I00	I,45±0,I0
^{98}Mo	2I	I,2	0,I30±0,006	6,9±0,3	0,056±0,004
^{144}Ce	22	I,I	I,0±0,I	2,6±0,3	-
^{129}I	23	I,0	27±3	36±4	0,I84±0,0I2
^{100}Mo	24	0,9	0,I99±0,003	3,75±0,I5	0,055±0,0I0
^{141}Pr	25	0,9	II,5±0,3	I7,4±2,0	0,073±0,0II

[1] (Accumulated to importance of its contribution.)

[*] The thermal cross-section and resonance integral are calculated from the resonance parameters.

cross-sections in the CFRMF assembly [6], the neutron spectrum of which is similar to that of fast reactors.

Since the evaluations in Refs [1-4] were completed, a lot of experimental data on fast neutron capture cross-sections have been published, which are characterized by the use of increasingly sophisticated techniques for cross-section measurements, more accurate methods for taking account of the background associated with neutron capture, and reliable cross-section absolutization. An analysis of such data was made in Refs [7-10]. In the course of this analysis the results of earlier measurements carried out using relative methods [8, 10] were also renormalized on the basis of the latest standards. As a result of this renormalization many discrepancies in the

experimental data were eliminated, as were differences between the results of earlier measurements and those of more recent experiments. The data thus selected were used as a basis for the present evaluation of neutron capture cross-sections.

The main criteria for establishing recommended files of evaluated neutron cross-sections are summarized below.

First, new values of the neutron resonance parameters [5] were used for the resolved resonance region, with a negative resonance usually being introduced to describe the thermal neutron capture cross-sections. The upper limit of the resolved resonances was determined from the condition that too many resonances should not be omitted.

Secondly, an unresolved resonance region with an upper limit of 30-100 keV was used for the majority of isotopes. For this region energy-dependent average neutron and radiation widths were included which were obtained with the help of the EVPAR program [7] from the condition for the optimal description of existing experimental data on average resolved resonance parameters and fast neutron radiative capture cross-sections in the energy range 1-100 keV.

Thirdly, in the energy range above 100 keV, the capture cross-section evaluations were based on a statistical description of selected experimental data [8, 9]. For 1-8 MeV neutron energy range, for which practically no experimental data are available, earlier cross-section evaluations were widely used [3, 4]. However, for the energy range above 8 MeV, a new evaluation based on the empirical systematics of experimental data in the direct collective neutron capture model was employed for all isotopes [10].

Fourthly, evaluations from the JENDL or ENDF/B-V libraries were utilized for elastic and inelastic scattering cross-sections and for the total neutron cross-sections above the unresolved resonance region. The criterion for selecting the appropriate evaluation was that its neutron inelastic scattering cross-sections should agree with the EVPAR program calculations.

Table 2. Characteristics of fission product evaluations included in the library of recommended evaluated neutron data

Isotope	Ranking of fission product (acc. to importance of contribution)	Number of resonances	$E^{max*}_{res.}$ keV	$E^{max*2}_{unres.}$ keV	$\langle\sigma_c\rangle^{*3}$, b	Evaluation used		Error of capture cross-sections, %
						Capture	Scattering	
^{95}Mo	18	55	2,0	100	-	JENDL-II	JENDL-II	15
^{97}Mo	12	64	1,8	100	-	JENDL-II	JENDL-II	15
^{98}Mo	21	161	32	100	-	JENDL-II	JENDL-II	20
^{100}Mo	24	158	26	100	-	JENDL-II	JENDL-II	20
^{99}Tc	2	107	1,4	141	0,348	FEhI**4	ENDF/B-V	10
^{101}Ru	3	40	1,0	120	-	"	ENDF/B-V	10
^{102}Ru	10	8	1,3	100	0,102	"	JENDL-I	10
^{104}Ru	19	8	1,2	100	0,100	"	JENDL-I	10
^{106}Ru	14	-	0,5	-	-	JENDL-I*3	JENDL-I	30
^{103}Rh	5	164	2,0	92	0,405	FEhI**4	JENDL-I	15
^{105}Pd	1	199	2,0	283	-	"	ENDF/B-V	10
^{107}Pd	4	60	0,7	300	-	"	ENDF/B-V	15
^{109}Ag	13	64	1,0	132	0,408	"	ENDF/B-V	10
^{129}I	23	5	2,0	500	-	"	JENDL-I	20
^{131}Xe	16	39	1,0	164	-	"	JENDL-I	25
^{133}Cs	6	160	3,5	-	0,292	JENDL-I	JENDL-I	10
^{135}Cs	11	-	0,03	-	-	JENDL-I*3	JENDL-I	30
^{141}Pr	25	15	0,99	-	0,080	ENDF/B-V	ENDF/B-V	10
^{144}Ce	22	-	0,5	-	-	JENDL-I*3	JENDL-I	30
^{143}Nd	15	65	2,5	30	-	FEhI**4	JENDL-I	20
^{145}Nd	9	114	2,0	30	-	"	JENDL-I	20
^{147}Pm	7	43	0,30	100	0,743	"	JENDL-I	25
^{147}Sm	46	120	0,75	120	-	"	JENDL-I	20
^{149}Sm	8	70	0,12	520	-	"	JENDL-I	20
^{151}Sm	17	76	0,10	10	-	"	JENDL-I	30
^{151}Eu	-	92	0,01	10	2,31	ENDF/B-V	ENDF/B-V	15
^{153}Eu	20	72	0,01	10	1,44	ENDF/B-V	ENDF/B-V	15

[*] Upper limit of resolved resonance region.

[*2] Upper limit of unresolved resonance region.

[*3] Renormalized cross-section region.

[*4] Power Physics Institute, Obninsk.

As no new experimental data on the excitation functions of low-lying levels have appeared in the past few years, there is a need to increase the accuracy of existing neutron inelastic scattering cross-section evaluations. Evaluations of threshold reaction cross-sections were taken from the ENDF/B-V files without modification, since possible errors would be insignificant for reactor applications.

Table 2 shows the number of neutron resonances included in the files, the limits of the resolved and unresolved resonance regions and the

recommended evaluations of capture and scattering cross-sections; also indicated are the average neutron capture cross-sections calculated from file data for the spectrum of the CFRMF assembly and the errors of the recommended capture cross-sections determined from the variance of the experimental data and the discrepancies that exist in the average cross-section evaluations in the 10-300 keV neutron energy range. Table 3 shows the parameters of the statistical description used for capture cross-sections: the average spacing between S-resonances D_S, the neutron strength functions of S-, P- and D-waves, the radiation strength function $S_\gamma = \Gamma_\gamma / D_S$ and the potential scattering radius R'. By comparing the cross-sections calculated for the spectrum of the CFRMF assembly with the data from Table 1, it can be concluded that, within the error limits the evaluations are in agreement with the integral

Table 3. Average neutron resonance parameters used in the statistical description of recommended neutron capture cross-sections

Isotope	D_S, eV	$S_0 \cdot 10^{-4}$	$S_1 \cdot 10^{-4}$	$S_2 \cdot 10^{-4}$	$S_\gamma \cdot 10^{-4}$	R', fm
^{95}Mo	80,0	0,37	5,48	3,65	29	6,70
^{97}Mo	60,0	0,37	5,48	3,65	30	6,67
^{98}Mo	950	0,37	5,48	3,65	I,40	6,66
^{100}Mo	620	0,37	5,48	3,65	I3,7	6,64
^{99}Tc	26,0	0,48	6,60	0,20	80	6,0
^{101}Ru	I5,0	0,59	6,I0	0,25	I00	6,4
^{102}Ru	280	0,55	5,00	0,55	3,2	6,6
^{104}Ru	300	0,33	6,04	0,33	2,8	6,7
^{106}Ru	I000	0,33	5,80	-	I,5	6,4
^{103}Rh	I6,0	0,53	5,50	0,53	60	6,2
^{105}Pd	I0,0	0,54	5,60	0,54	I40	6,I
^{107}Pd	II,4	0,60	5,80	0,60	I70	6,6
^{109}Ag	I8,7	0,68	3,80	0,68	50	6,6
^{129}I	25,0	0,80	2,00	0,80	40	5,6
^{131}Xe	50,0	I,20	I,80	I,20	24	5,95
^{133}Cs	23,2	I,42	I,39	-	5I	5,2
^{135}Cs	60,0	I,6I	I,26	-	-	5,2
^{141}Pr	88,0	I,50	-	-	-	6,28
^{144}Ce	I000	2,97	0,78	-	-	4,6
^{143}Nd	36,0	3,20	0,80	I,60	25	5,8
^{145}Nd	I7,0	4,40	0,70	2,20	45	6,5
^{147}Pm	3,7	3,00	0,60	3,00	I90	7,I
^{147}Sm	5,I	4,70	I,00	2,00	I50	8,3
^{149}Sm	I,9	4,80	0,50	4,80	337	7,5
^{151}Sm	I,0	3,40	0,50	2,00	950	8,0
^{151}Eu	0,59	4,07	0,80	-	I650	8,8
^{153}Eu	I,37	2,50	0,60	-	700	8,8

experiments for the majority of nuclei. The isotopes ^{99}Tc and ^{109}Ag are an exception, since for them the discrepancies significantly exceed the error levels indicated. We shall revert to these discrepancies after briefly reviewing the evaluations of the errors of the capture cross-sections used.

The capture cross-section evaluations for molybdenum isotopes [11] are mainly based on the measurement results from Ref. [12], which correspond adequately to earlier lead cube measurements [13]. These data are not contradicted by the results of the large number of activation measurements [10] which are available for the isotopes ^{98}Mo and ^{100}Mo. The data as a whole allow an error of 20% to be assigned to the fast neutron capture cross-section evaluations, a figure which roughly corresponds to that of the experimental data [12].

Experimental data used in capture cross-section evaluations for the isotopes ^{103}Rh, ^{105}Pd, ^{133}Cs and ^{141}Pr have a relatively high level of consistency, and the discrepancy between evaluations is no more than 10%. This discrepancy is clearly the optimal determination of the error of the recommended fast neutron capture cross-section evaluation. The situation regarding ^{109}Ag is rather more complex, as the spread of the experimental data and the discrepancies between evaluations are greater (Fig. 1(a)). However, the good agreement shown by the results of recent experiments on linear accelerators [14] - on which the present evaluation was based - enable an error of 10% to be ascribed to the evaluation, and this is in line with the measurement error. The evaluation for the isotopes ^{99}Tc, ^{101,102,104}Ru (Fig. 1(b)) is also based on more recent experimental data [15, 16] than were previous evaluations. Since for the first two istopes these data agree quite well with the statistical description based on average resolved resonance parameters, the evaluation of the capture cross-section for these isotopes can be assigned the same error as the experimental data [15, 16]. The same error can be used for ^{102,104}Ru also, although it is harder to justify this as the

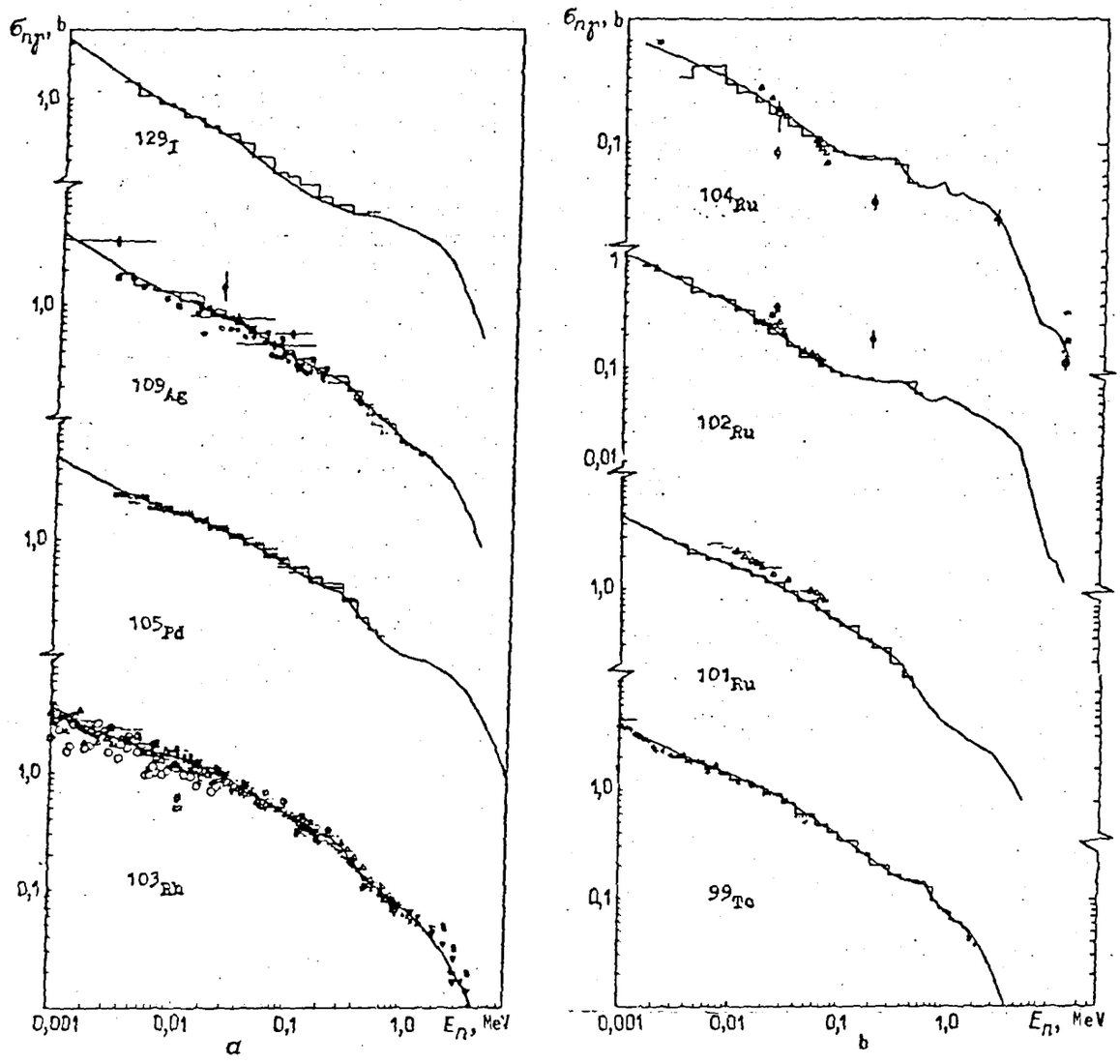

Fig. 1. Experimental data on fast neutron radiative capture cross-sections (histograms and points [10]) and their description by recommended evaluations (continuous lines) for various isotopes (a,b).

information on neutron resonance parameters is less comprehensive than for the odd isotope of ruthenium.

The capture cross-section evaluations for the isotopes ^{107}Pd and ^{129}I are based on recently obtained experimental data [17, 18]. The difficulties involved in preparing unstable isotope targets raise many questions concerning possible systematic errors in these measurements, which have been performed only once. The cross-section evaluations and experimental data for these isotopes can therefore hardly be assigned an error of less

than 20%, but a final answer will have to wait until the cross-section measurement has been repeated.

Experimental data are not available on fast neutron capture for ^{131}Xe, ^{147}Pm and ^{151}Sm and all cross-section evaluations are based on optical-statistical calculations of cross-sections with strength functions derived from analysing resolved resonances. Differences in evaluations are on average 30%, and this should clearly be taken as the error of the recommended evaluations. There are no experimental data for the isotopes ^{106}Ru, ^{135}Cs and ^{144}Ce for either the fast neutron capture cross-sections or the average neutron resonance parameters. There are discrepancies of more than a factor of 2 between the various evaluations for these isotopes (Fig. 2). The evaluations recommended by the authors are based on the systematics of the isotopic dependences of fast neutron capture cross-sections [8], and the errors associated with these systematics are comparable with those of cross-section evaluations which use average resonance parameters, i.e. they are not less than 30%, but on average do not significantly exceed this figure.

Determining the error of capture cross-section evaluations is a complex task for the isotopes ^{143,145}Nd and ^{147,149}Sm, where the discrepancies in the experimental data are both substantial and difficult to explain (Fig. 3) [9, 19]. There are also significant discrepancies for these isotopes in the radiation strength functions obtained from the description of observed capture cross-sections and the analysis of average resolved resonance parameters. A critical attitude should therefore be adopted to the errors indicated by the authors for the experimental data. It would thus be realistic at present to assume an error of 20%, which is approximately twice as high as the measurement errors given in the original papers. The odd isotopes of neodymium and samarium undoubtedly require further work on the measurement and analysis of fast neutron capture cross-sections in order to eliminate the current discrepancies in the experimental data.

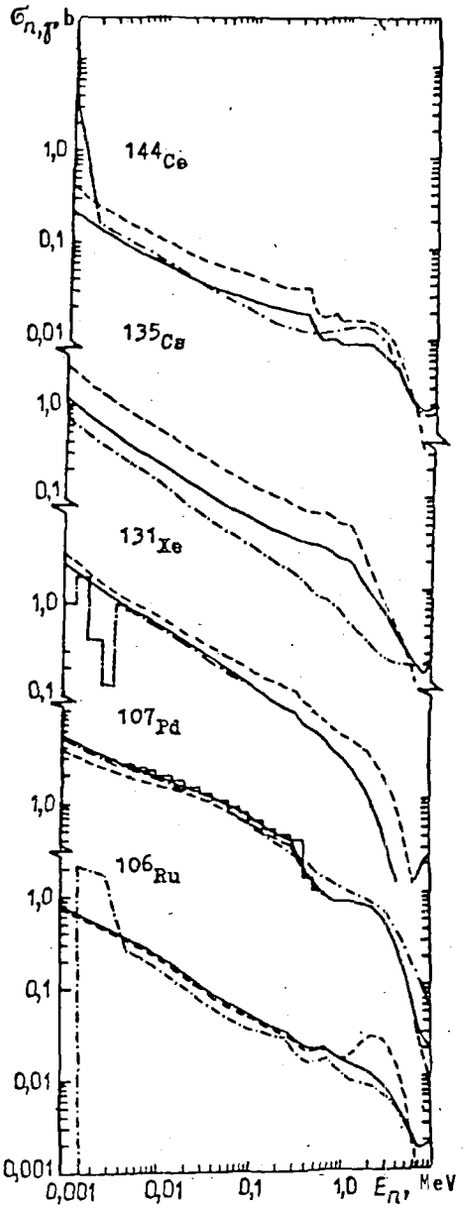

Fig. 2.

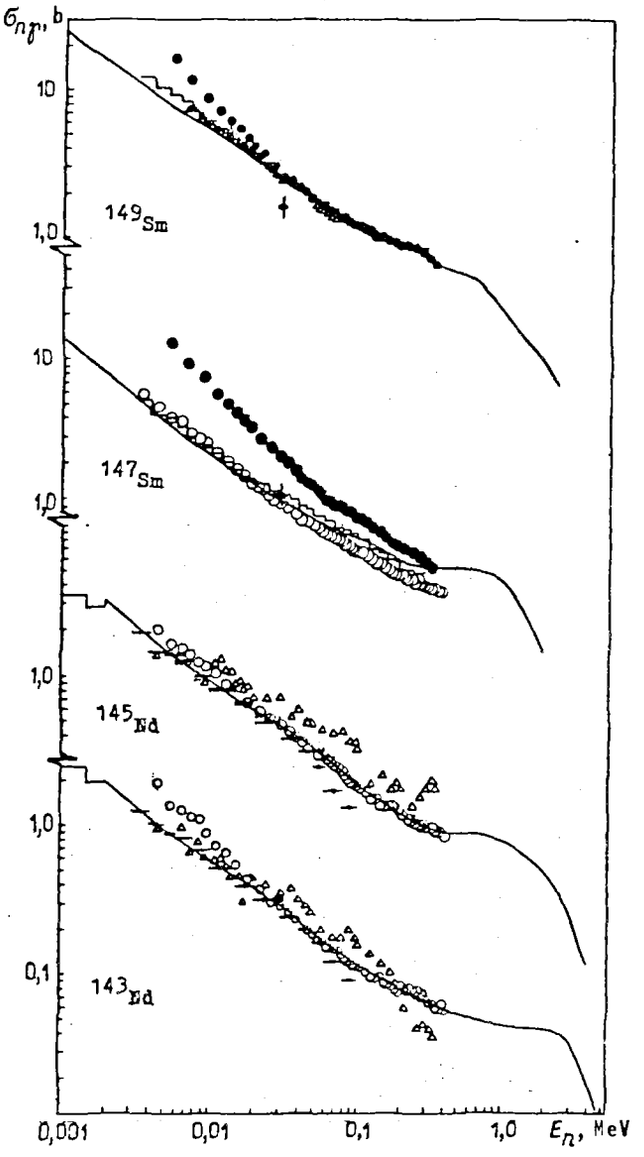

Fig. 3.

Fig. 2. Comparison of recommended evaluations (continuous curve) with ENDF/B-V (dashed curve) and JENDL-1 (dot-dash curve) evaluations of isotopes for which no experimental data are available. The results of recent measurements [17] for ^{107}Pd are shown in the histogram.

Fig. 3. Comparison of recommended evaluations (continuous curve) with experimental data (points and histograms) for odd isotopes of neodymium and samarium.

The above discussion of errors shows that the recommended capture evaluations for the first ten most important fission products - which are responsible for over 50% of fast reactor core poisoning - are accurate to within 10-15%. Since when calculating for an effective pseudo fragment the independent errors of the cross-sections of individual products vanish statistically, it can be expected that the error of the pseudo-fragment

capture cross-sections predicted on the basis of the recommended files will not exceed 10%, i.e. it will satisfy current requirements for the accuracy of fission product evaluation [20].

It should be noted that inconsistencies between differential and integral measurement data are also relevant to the question of discrepancies between calculated average cross-sections and the data for the CFRMF assembly. It is clear that further measurements - and particularly integral measurements - will have to be made. It would also be of interest to seek ways of checking evaluations of capture cross-sections for isotopes for which experimental data are not available.

REFERENCES

[1] FORT, E., KREBS, J., RIBON, P., et al., in: Nejtronnaya Fizika: Proc. 4th All-Union Conference on Neutron Physics, Kiev, 18-22 April 1977, Part 4, TsNIIatominform, Moscow (1977) 3 (in Russian).

[2] GRUPPELAAR, H., Rep. ECN-13 (1977); ECN-33 (1977); ECN-65 (1979).

[3] KIKUCHI, Y., NAKAGAWA, T., MATSUNOBU, H., et al., Rep. JAERI-1268 (1981).

[4] SCHENTER, R.E., ENGLAND, T.R., in: Proc. specialists' meeting on neutron cross-sections of fission product nuclei, Bologna (1979) 273.

[5] MUGHABGHAB, S.F., DIVADEENAM, H., HOLDEN, N.E. Neutron cross-sections, 1, Part A, N.Y.: Academic Press (1981); MUGHABGHAB, S.F., ibid, Part B (1984).

[6] HARKER, Y.D., ROGERS, J.W., MILLSAP, D.A., Rep. TREE-1259 (1978).

[7] YURLOV, B.D., BELANOVA, T.S., IGNATYUK, A.V., et al., Vopr. At. Nauki i Tekh., Ser. Yad. Konst., 50 (1) (1983) 25 (in Russian).

[8] BELANOVA, T.S., GORBACHEVA, L.B., GRUDZEVICH, O.T., et al., At. Ehnerg., 57 (1984) 243 (in Russian).

[9] ZAKHAROVA, S.M., ABAGYAN, L.P., KAPUSTINA, V.F. ^{147,149}Sm Isotopes, Obninsk (1984) (in Russian).

[10] BELANOVA, T.S., IGNATYUK, A.V., PASHCHENKO, A.B., PLYASKIN, V.I. Neutron Radiative Capture, Ehnergoatomizdat, Moscow (1986) (in Russian).

[11] KIKUCHI, Y., TOGAWA, O., WATANABE, T., et al., Rep. JAERI-M84-103 (1984).

[12] MUSGROVE, A.R., ALLEN, B.J., BOLDEMAN, J.W., MACKLIN, R.L., Nucl. Phys. (1976), A270, 108.

[13] KAPCHIGASHEV, S.P., POPOV, Yu.P., At. Ehnerg., 15 (1963) 120 (in Russian).

[14] MACKLIN, R., Nucl. Sci. and Eng. 82 (1982) 400; MIZUMOTO, M., ASAMI, A., NAKAJAMA, Y., et al., in: Nucl. data for sci. and technol.: Proc. on the Intern. Conf. Antwerp (1982), Holland (1983) 226.

[15] MACKLIN, R., Nucl. Sci. and Eng. 81 (1982) 520.

[16] MACKLIN, R., WINTERS, R., HALPERIN, J., ibid. 73 (1980) 174.

[17] MACKLIN, R., ibid. 89 (1985) 79.

[18] MACKLIN, R., ibid. 85 (1983) 350.

[19] BOKHOVKO, M.V., KAZAKOV, L.E., KOHOHOV, V.E., et al., Vopr. At. Nauki i Tekh. Ser. Yad. Konst. 3 (1985) 12.

[20] MANOKHIN, V.N., YSACHEV, L.N., At. Ehnerg. 57 (1984) 234.

NUCLEAR DATA LIBRARIES USED AT THE SHKODA POWER ENGINEERING PLANT

Ya. Khep, V. Valenta

In 1970, the Shkoda Power Engineering Plant was given the task of establishing a set of programs for evaluating the radiation situation at nuclear power plants with WWER reactors during normal operation and under accident conditions. This task involved a considerable amount of work, which is described below.

1. Determination of sources of radiation:
   - In spent fuel as a result of the decay of fission products and actinides and also as a result of spontaneous fission, fission and the (α,n) reaction in oxygen;
   - In the coolant: activation products of the coolant and its impurities and also corrosion and fission products;
   - Activated parts (structural materials, air in the reactor cavity, and so on).
2. Study of radioactivity at nuclear power plants and application of various methods for its removal.
3. Determination of the dose equivalent to workers and the public.

In order to carry out these tasks, it was necessary to analyse the relevant reference data and set up libraries, since none existed on magnetic media. The data were arranged in three libraries.

First, the BIBA library [1] of radioactive products is used to calculate the balances of activities and radiation sources resulting from the decay of corrosion products in the primary circuit, activation products in the coolant and its impurities, activation products in structural materials and so on. The library contains data for 828 nuclides, with atomic numbers 1-84, which are found in the natural isotopic mixture of the relevant element or occur as a result of activation and radioactive decay. The following information is given for each nuclide in the library: a definition of the

nuclide - its number in the library, its atomic number, mass number and characteristics of state; the proportion of the nuclide in the natural mixture - the number of nuclei in 1 g of the element; the radioactive decay characteristics - the decay constant, a description of the shape of the decay chain (the number of final nuclides and corresponding transition probabilities); the characteristics of transition as a result of activation reactions - the type of reaction (five types of reaction are taken into account - (n,γ), (n,p), (n,n'), (n,α), $(n,2n)$), the corresponding cross-sections (in two neutron groups), the number of final nuclides and transition probabilities; the characteristics of the radioactive nuclides - number of γ-lines, β^- or β^+-spectra, the energy of the discrete lines (or average energies of the β-spectra) per decay and the corresponding yields per decay.

Secondly, the BIBGRFP library of fission products is used to calculate the balance of radioactivities and fission product radiation sources in fuel elements, in the primary circuit, in the nuclear power plant area and so on. The library contains data for 584 fission products (elements with atomic numbers 29-67). The following information is given for each nuclide in the library: a definition of the nuclide - its number in the library, its atomic number, mass number and characteristics of state; independent fission yields for ^{235}U, ^{239}Pu, ^{241}Pu and ^{238}U (induced by thermal and 1 MeV neutrons); radioactive decay characteristics - the decay constant and a description of the shape of the decay chain (the number of the final nuclide and the corresponding transition probability); the characteristics of transition as a result of the (n,γ) reaction - the reaction cross-section (for thermal neutrons) and the resonance integral and a description of the type of transition (the number of final nuclides and corresponding transition probabilities). The energy sources resulting from radioactive decay are sources of α- and β-radiation per decay, and also sources of γ-radiation in two group systems:

- The 13-group system - the distribution of the group boundaries corresponds to the SOPRGA programs set [2] for calculating dose equivalents from sources with different (elementary) geometrical configurations;
- The 12-group system corresponding - in terms of distribution - to Sneider data groups for calculating dose equivalents to man during decay in organs or in the ambient air.

Thirdly, the BIPAL library [3] of actinides is used to solve the equation for the balance of actinides and the members of their decay chains. The library contains data for 113 nuclides from the heavy element region. The library provides the following information for each nuclide: a definition of the nuclide - its number in the library, its atomic number, mass number and characteristics of state; the proportion of the nuclide in the natural mixture of the corresponding element; radioactive decay characteristics - the decay constant and a description of the shape of the decay chain (the number of the final nuclides and corresponding probabilities); the characteristics of transition as a result of the (n,γ) reaction - the reaction cross-section (two neutron groups) and a description of the transition mode (the number of the final nuclides and corresponding transition probabilities); characteristics of the radioactive nuclides - the number of α-, γ-lines and β-spectra, the energy of the discrete lines (average energies of β-spectra) per decay and the corresponding yields per decay; characteristics of the fissionable nuclides - the fission cross-section (two groups), the fission threshold energy, the average number of neutrons per thermal-induced-fission neutron, the decay constant for spontaneous fission and the average number of neutrons per fission.

All the data contained in these libraries were taken from the literature or were recalculated on the basis of the literature (for example, the fission cross-sections, the independent fission yields and the group energy sources).

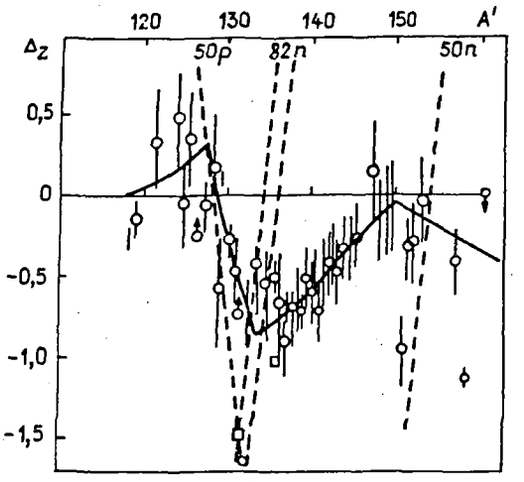

Fig. 1. Approximate deviation Δ_Z from even distribution [$\Delta_Z(A') = Z_p(A) - (Z_f/A_{fc})\ A'(A)$ where $A' \geq A_c/2$].

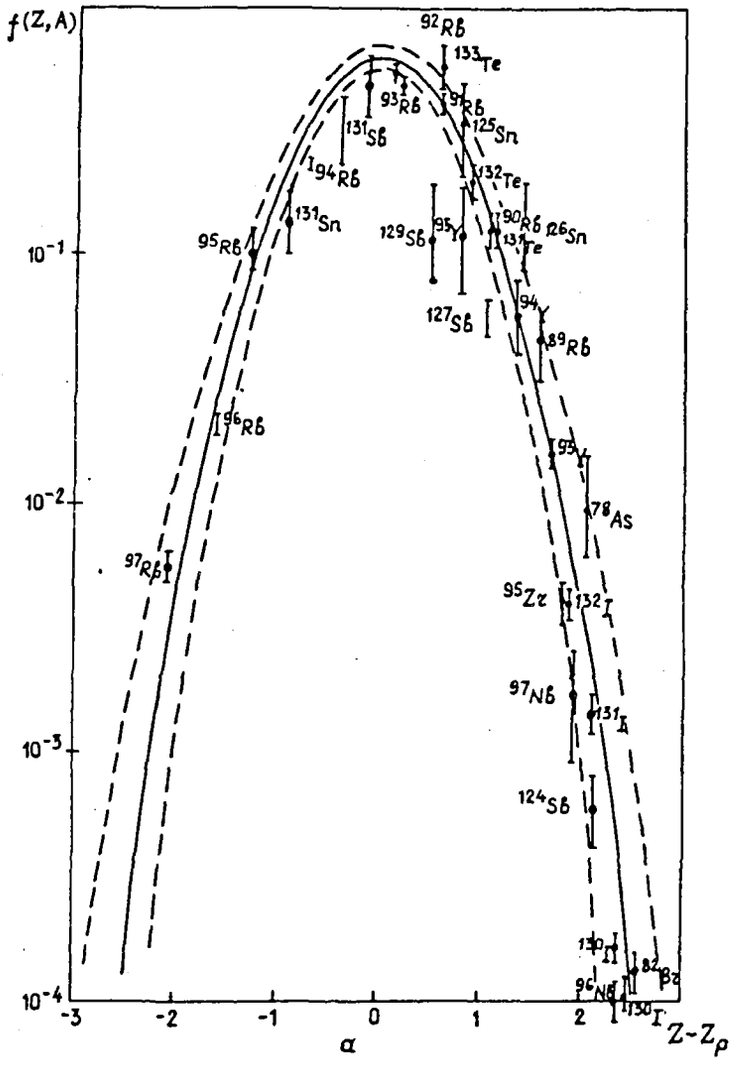

Fig. 2. Comparison of the experimental and calculated data on (a) the relative independent yield, (b) the cumulative yield, and (c) the relative cumulative yields for several mass numbers (------ [39]; □, Δ, O, Q - [40]) in thermal-neutron-induced fission of ^{235}U.

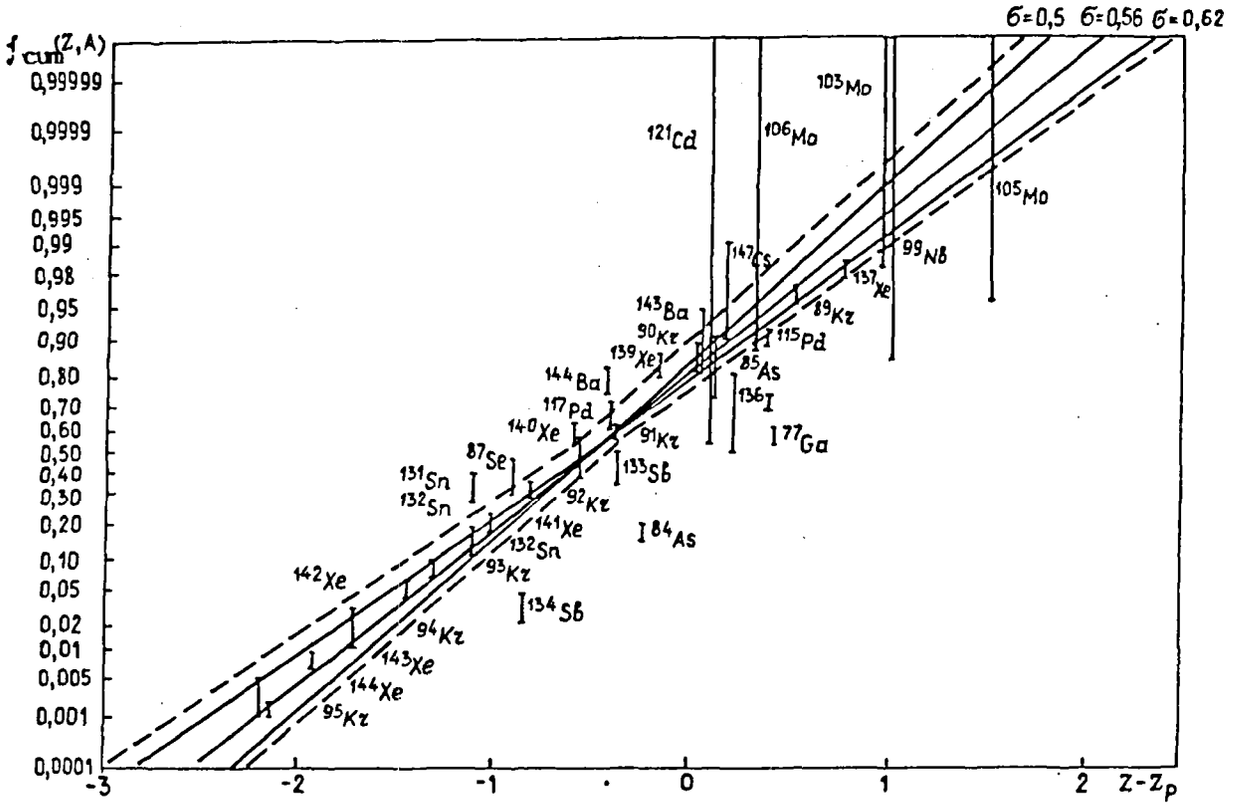
σ=0,5 σ=0,56 σ=0,62
$f_{cum}(Z,A)$
0,99999
0,9999
0,999
0,995
0,99
0,98
0,95
0,90
0,80
0,70
0,60
0,50
0,40
0,30
0,20
0,10
0,05
0,02
0,01
0,005
0,001
0,0001
-3
-2
-1
0
1
2
$Z-Z_p$
^{103}Mo
^{121}Cd
^{106}Mo
^{105}Mo
^{147}Cs
^{99}Nb
^{137}Xe
^{89}Kr
^{143}Ba
^{90}Kr
^{139}Xe
^{115}Pd
^{85}As
^{144}Ba
^{136}I
^{117}Pd
^{140}Xe
^{91}Kr
^{77}Ga
^{87}Se
^{133}Sb
^{131}Sn
^{132}Sn
^{92}Kr
^{84}As
^{141}Xe
^{132}Sn
^{142}Xe
^{93}Kr
^{134}Sb
^{94}Kr
^{143}Xe
^{144}Xe
^{95}Kr

Fig. 2 (b)

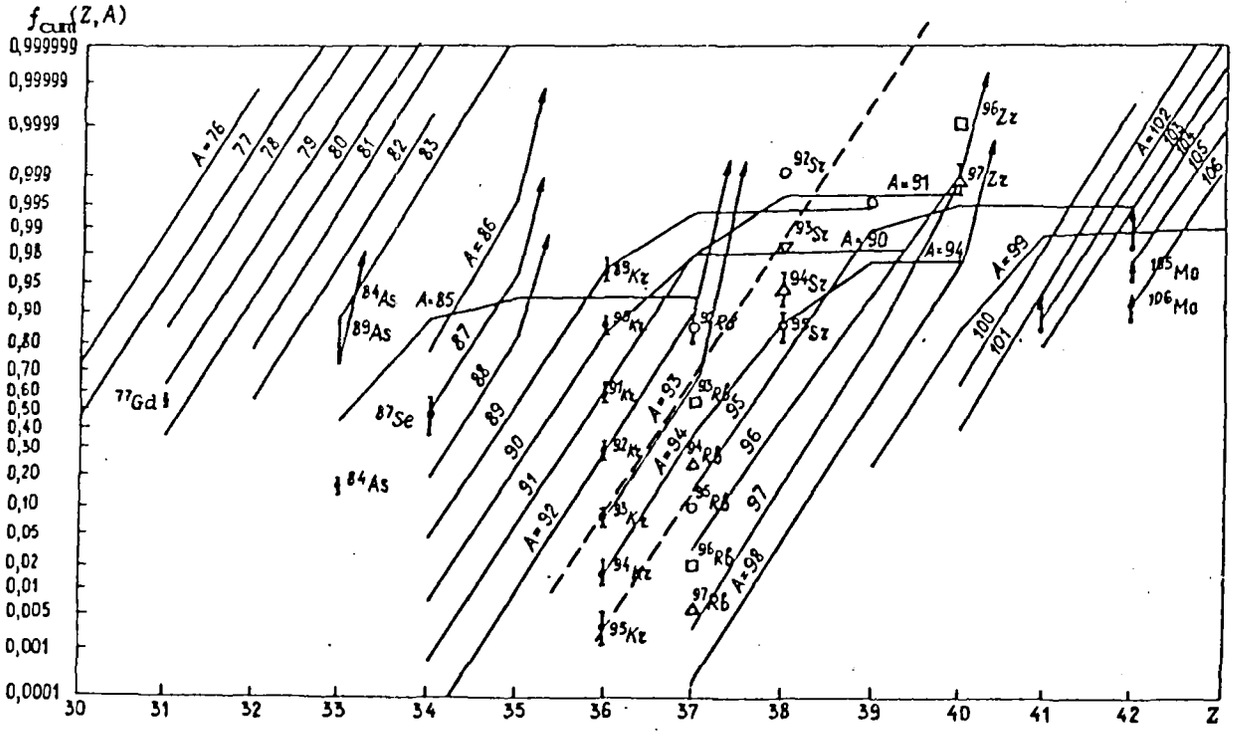
$f_{cum}(Z,A)$
0,999999
0,99999
0,9999
0,999
0,995
0,99
0,98
0,95
0,90
0,80
0,70
0,60
0,50
0,40
0,30
0,20
0,10
0,05
0,02
0,01
0,005
0,001
0,0001
30
31
32
33
34
35
36
37
38
39
40
41
42
Z
A=76
77
78
79
80
81
82
83
A=86
A=85
A=91
A=90
A=94
A=99
A=102
103
104
105
106
A=93
A=92
A=98
87
88
89
90
91
92
93
94
95
96
97
100
101
^{77}Gd
^{84}As
^{89}As
^{87}Se
^{84}As
^{89}Kr
^{96}Kr
^{91}Kr
^{92}Kr
^{93}Kr
^{94}Kr
^{95}Kr
^{92}Sr
^{93}Sr
^{94}Sr
^{95}Sr
^{96}Zr
^{97}Zr
^{95}Rb
^{96}Rb
^{97}Rb
^{105}Mo
^{106}Mo

Fig. 2 (c)

The literature used to compile the BIBA library was as follows: Refs [4-9] were used to calculate the decay constants and to determine the nuclide composition in the natural mixture of elements; Ref. [8] was used to calculate the shape of the decay chains; for the most part Refs [9-14] were used to determine the γ-line energies and yields (the limitation on the number of γ-lines (31) is determined by the basic principles of the library - for the majority of γ-emitters the number of γ-lines is less than 31; if some lines had to be left out because of this limitation, then low energy and low yield lines were disregarded; Refs [10 and 15] or [12-14] were used principally to determine the energy of the β-spectra; Refs [4 and 10] were used to determine the characteristics of the α-lines and Refs [14, 16-18] were used to determine the cross-sections.

The BIBGRFP library is based on data from the BIBFP library [19] and data on independent fission yields analysed in Ref. [20]. The BIBFR library is based on data from Refs [21-23]. For additional data on cross-sections, Refs [24 and 25] were used. Some corrections to the decay constants were made as a result of comparison made with data from Refs [4, 26]. The basis for determining the independent yields will be outlined later in the part describing the calculations.

The following literature was used to establish the BIPAL library: to select the nuclide set - Refs [27, 28]; to determine the main nuclide characteristics - Ref. [4] (half-life), [29] (half-life for spontaneous fission), [4, 28] (cross-sections), [30-32] (resonance integrals) and [10, 11, 33, 34] (energy sources for α-, β-, γ-decay).

Let us consider in more detail the problems of determining independent fission yields. The yields contained in the BIBGRFP library were taken from calculations in Refs [20, 35]. Since this library gives the independent yields for fission induced by thermal neutrons for ^{235}U, ^{239}Pu and ^{241}Pu and by neutrons of about 1 MeV for ^{235}U, ^{239}Pu, ^{241}Pu and ^{238}U,

isobaric yield data from Refs [23, 36] were used. It should be noted that Refs [20, 35]

describe the algorithm used to recalculate the isobaric yields for other energies and fissionable materials. This is based on the shift in the yields which is proportional to the change in the average mass of light and heavy fragments (in accordance with the data in Ref. [37]).

The independent fission yields are determined by the relationship

$$Y(Z,A)=Y(A)\frac{1}{\sigma(A)\sqrt{2\pi}}\int_{Z-\frac{1}{2}}^{Z+\frac{1}{2}}\exp\left\{-\frac{[Z'-Z_p(A)]^2}{2\sigma^2(A)}\right\}dZ'=$$

$$=Y(A)\left\{P\left[\frac{Z+\frac{1}{2}-Z_p(A)}{\sigma(A)}\right]-P\left[\frac{Z-\frac{1}{2}-Z_p(A)}{\sigma(A)}\right]\right\}=Y(A)f(Z,A), \qquad (1)$$

where Z,A are the atomic number and mass numbers of the isotope for which the independent yield Y(Z,A) is being calculated; Y(A) is the isobaric yield for the mass number A; $\sigma(A)$ is the Gauss distribution dispersion; $Z_p(A)$ is the most probable value of Z for the mass chain A; f(Z,A) is the relative independent yield.

The function P(x) was calculated using the expression in Ref. [38]. Equation (1) was used to determine the independent yields for

$$Z = Z_{min}^{(A)}+1, Z_{min}^{(A)}+2,\ldots,Z_{max}^{(A)}\ ; \qquad Y(Z_{min},A)=Y(A)-\sum_{Z=Z_{min}+1}^{Z_{max}}Y(Z,A),$$

where Z_{min}, Z_{max} are the minimum and maximum atomic numbers present in a chain with the mass number A.

When for an isotope with the numbers Z,A there are many nuclides (different isomeric states), it is assumed that the independent yield Y(Z,A) is divided into equal parts. The justification for this is the fact that data are not available for the spins of all the nuclide-isomers in the BIBGRFP library and therefore it is not possible to use the polyempirical equation from Ref. [39] to recalculate the yields. The following relationship is used in this calculation

$$Z_p(A)=\frac{Z_f}{A_{fc}}A'(A)+\Delta_Z(A')+\delta_Z(A).$$

where Z_f is the atomic number of the fissionable material; A_{fc} is the mass number of the compound nucleus; $A_z(A)$ is the deviation from even charge distribution; $\delta_z(A)$ is the correction for anomalous values of Z_p (in the calculations $\delta_z(A) = 0$ was used); $A'(A) = A + \nu_p(A)$, where A is the fragment mass after emission of prompt neutrons; $\nu_p(A)$ is the average number of neutrons emitted by the fragment. The $\nu_p(A)$ data for thermal- neutron-induced fission of ^{235}U are taken from Ref. [40]. From the diagrams in Ref. [41] we can conclude that the shape of the function $\nu_p(A)$ is similar for various fissionable materials and that the shift in the curves $\nu_p(A)$ is proportional to the shift in the average masses of the heavy and light fragments [*] (the effect of the energy can be taken into account in this way).

The dependence $\Delta_z(A')$ was approximated on the basis of the results of Ref. [43] (Fig. 1) for each section of the linear function (Table 1).

For $A' < A_c/2$ the antisymmetry of the function $\Delta_z(A')$ relative to $A_c/2$ was used [for $A' < A_c/2$ let us say that $B = (A_c/2) - A'$ and $\Delta_z(A') = -\Delta_z(A_c/2 + B)$]. The following expression was used to determine $\sigma(A)$:

$$\sigma_f(A, E_n) = 0{,}56 + \left\{\sqrt{\frac{A_c T_f}{16\beta}} - \sqrt{\frac{236\, T_{236}}{16\beta}}\right\} + \delta_\sigma(A), \qquad (2)$$

where E_n is the energy of the fission-inducing neutron; A_c is the mass of the compound nucleus; f is the index of fissionable material; $\beta = 19.307$ MeV [the coefficient of the expression $(A-2Z/A)^2$ in the Weizsäcker equation for the binding energy]; $\delta_\sigma(A)$ is the correction for shell effects (this term can be determined from a comparison with experimental data); let us suppose that $\delta_\sigma(A) = 0$ [**]; T_f, T_{236} is the temperature of the compound nucleus f and ^{236}U determined [44, 45] from

---

[*] Equations from Ref. [42] were used to determine the average masses of light and heavy fragments.

[**] According to expression (2), the value of σ does not depend on A when $\delta_\sigma(A) = 0$.

Table 1

$\Delta_Z(A')$ at the boundary points of the range

Range	Range boundary Lower	Upper
$A'\varepsilon < A_c/2, 128 >$	0	0.3
$A'\varepsilon < 128, 134 >$	0.3	-0.8
$A'\varepsilon < 134, 150 >$	-0.8	-0.05
$A'\varepsilon < 150, 165 >$	-0.05	-0.5

Note: A_c is the mass of the compound nucleus.

Table 2

Dispersion of the compound nucleus

E, MeV	T_f, MeV	σ
0.025 E-6	0.417	0.56
1	0.446	0.58
10	0.645	0.695
14	0.719	0.738

the relationship $I/T = \sqrt{a/u} - 5/4u$, in which $a = 0.16\ A_c$; $u = E_f^n + E_k^n - E_f^{prah} > 0$, where E_f^n is the neutron binding energy in the compound nucleus; E_k^n is the kinetic neutron energy; E_f^{prah} is the fission barrier of the compound nucleus.

In determining $\sigma(A)$ equation (2) was used in order to describe the dependence of σ on the type of fissionable material and on the neutron energy in accordance with statistical theory [46] and in order to obtain the value $\sigma = 0.56$ given in Ref. [40] for thermal neutron fission fission of ^{235}U. The dependence of the dispersion values obtained on energy in the case of ^{235}U fission and on the temperature of the compound nucleus is shown in Table 2.

The dispersion for thermal-neutron-induced fission of various fissionable materials is as follows: ^{235}U - 0.56; ^{239}Pu - 0.564; ^{241}Pu - 0.566.

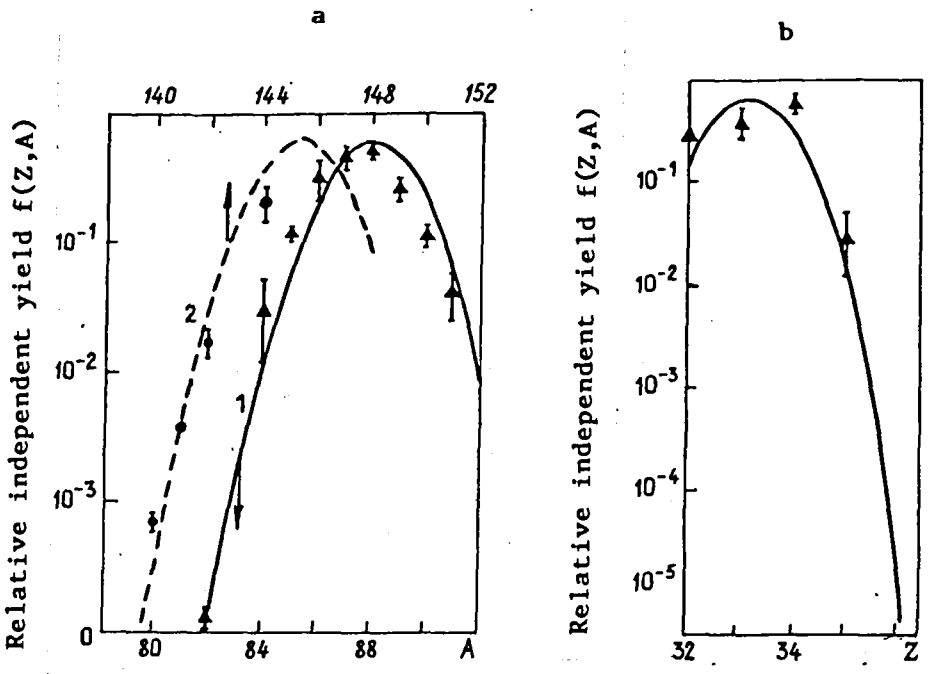

Fig. 3. Comparison of experimental and calculated relative independent yields as a function of (a) the mass number A for ^{35}Br (curve 1) ^{57}La (curve 2) and (b) the atomic number Z for A = 84.

Particular attention was given to the comparison of the yield data calculated by us with the experimental results (Figs 1-3). A comparison was made of all the data available in the literature [43, 47-52].

In accordance with Ref. [52] it seems that it is necessary to introduce a correction $\delta_\sigma(A,Z)$ in isobaric chains, which could take the following form, for example:

$$\delta_\sigma(A,Z) = 1/2\left[1+(-1)^A\right](-1)^Z\delta_\sigma ,$$

where $\delta_\sigma = 0.11$.

Even-even effects can be described by the relationship $\delta_\sigma = \delta A^{3/4}$, with the value $\delta = 0.00376$ being determined from a comparison of the experimental data (Fig. 4).

The results for independent yields given in the BIBGRFP library can be refined by:

- Using the correction $\delta_\sigma(Z,A)$ for even numbers of A (as was shown above);
- Replacing a Gauss distribution which is continuous in respect of the number Z by a discrete one. The Gauss distribution exists in

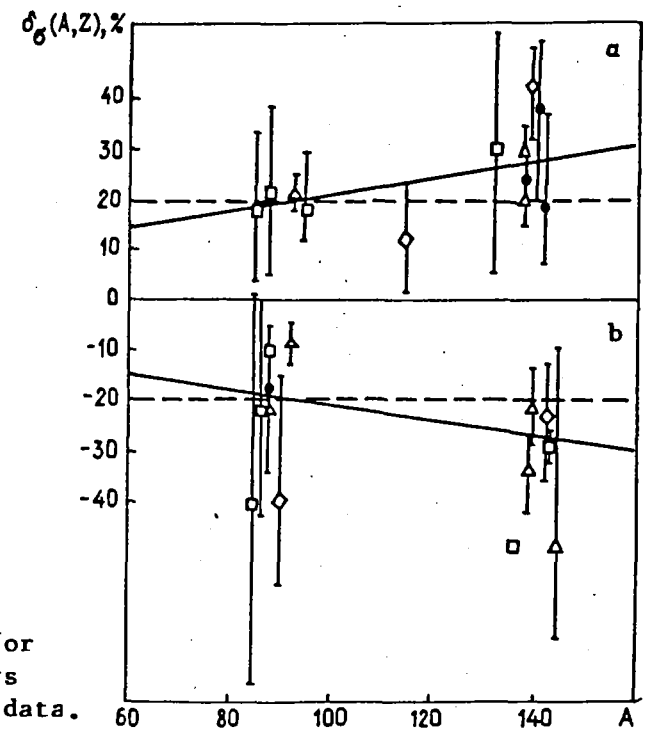

Fig. 4. Correction for dispersion for (a) odd and (b) even numbers of Z based on experimental data.

the range $(Z-Z_p) \in (-\infty, +\infty)$. In fact, the number Z is limited on the one side by stable nuclides, and on the other by the neutron instability curve. In addition, for even numbers of A it is necessary to use two types of distribution with different values for $\sigma(Z,A)$ as stated above. This means that an isobaric yield distribution occurs for a small number of nuclides with different numbers for Z;

- Including the correct independent yield distribution among the nuclide-isomer states of the same isotope, i.e. by using Gusev's polyempirical formula [39].

In order to calculate the balance of nuclides and proportional values, three libraries, which have gradually been built up over the past 14 years, are currently being used. There are plans to combine the data from the individual libraries to create a NITRITION library with a single data format for all nuclides. The data describing the energy sources (α-, γ-lines and β-spectra) will be replaced by group sources of γ-radiation and the average energy of charged particles per decay, as required by the programs; additions will be made to take account of evaluations of the effect of

radioactivity on the population (dose factors for external exposure from semi-infinite space, surface and so on).

So far, the NITRITION library contains 1180 nuclides with the numbers Z = 1-100. A first selection has been made of nuclides that appear simultaneously in two libraries (the main selection criterion being the quality of the reference sources). For the library to be used more widely, the accuracy of some of the cross-section data will have to be improved. In addition, the description of the activation reactions in the 2-group system is rather imprecise. Since the library is intended to be used for engineering calculations, it would be useful to employ the 26-group division (BNAB). The 128-group data from the Australian fission product library [53] for 192 nuclides have already been converted to this system (they are not yet included in the BIBGRFP). It would be useful to verify the data from the Australian library. It is possible that information on other nuclides may also need to be supplemented.

REFERENCES

1. Královcová E., Hep J., Valenta V. BIBA3 - Knihovna pro výpočet aktivací: Ae 5576/Dok., 1984.
2. Hep J., Valenta V., Smutný V., Královcová E. Anotace souboru programů TRABAK a SOPRGA: Ae 5208/Dok., 1984.
3. Královcová E., Hep J. Valenta V. BIPAL3 - Nová verze knihovny pro výpočty vyhořiváni štěpných materiálů a produktů jejich rozpadu: Ae 4702/Dok., 1981.
4. Seemann-Eggebert W. e.a. Nuklidkarte, Kernforschungzentrum Karlsruhe, 4. Auflage, 1974; 5. Auflage, 1981.
5. Zijp W.L. Nuclear data guide for reactor neutron metrology: ECN-37, 1978.
6. Zijp W.L., Baard J.H. Nuclear data guide for reactor neutron metrology, part 1-ECN-70, 1979; part 2-ECN-71, 1979.
7. Minoru Okada. Chart of nuclides relating to neutron activation: JAERI-M 9649, 1981.
8. Gusev N.G., Dmitriev P.P. Radioactive chains, Moscow (1978) (in Russian).
9. Gusev N.G., Dmitriev P.P. Quantum radiation of radioactive nuclides, Moscow (1977) (in Russian).
10. Nemets O.F., Gofman J.V. Nuclear physics handbook, Kiev (1975) (in Russian).
11. Meixner Ch. Gamma-energien, 2.Auflage, teil 1. Jülich: Jül-1087-RX, 1974.
12. Martin M.J. (edit). Nuclear decay data for selected radionuclides ORNL-5114, 1976.
13. Kocher D.C. Nuclear decay data for radionuclides in routine releases from nuclear fuel cycle facilities: ORNL (NUREG) TM-102, 1977.
14. Nichols A.L. Radioactive - nuclide decay data for reactor calculations. Activation products and related isotopes: AERE-R 8903. Harwell, Oxfordshire, 1977.
15. Kolobashkin V.M. et al. Beta radiation of fission products, Moscow (1978) (in Russian).
16. Handbook of nuclear activation cross-sections. Vienna: IAEA, 1974.
17. Jimenez. Section eficaces (n,γ), (n,α)y(n,2n) de los components de los aceros y otros materiales nucleaires. Madrid, 1972.

18.Pearlstein. J. Nucl. Energy, 1973, v.27, p.81.
19.Valenta V., Hep J. Fission product data library BIBFP: ZJE-158, 1975.
20.Valenta V., Hep J. Fission product yields: ZJE-211, 1978.
21.Blachot J., De Tourreil R. Bibliothèque de donnéss nucléaires relatives aux products de fission (3 éme edition): Note CEA-N-1526, 1972.
22.Barre B., De Tourreil R. Bibliothèque de donnéss nucléaires relatives aux products de fission (2 éme version): Note CEA-N-1423, 1971.
23. Barre B., De Tourreil R. Concentration des produits de fission après une fission thermique de ^{235}U et ^{239}Pu at après une fission rapid (E ~ 1 MeV) de ^{235}U, ^{238}U et ^{239}Pu: Note CEA-N-1309, 1970.
24.Rychelynk J. Capture des produits de fission: Rap. SPM 936, 1969.
25.Sakata, Nagayama, Otake. Study for decay chain of fission products: JAERI-1194, 1970.
26.Blachot J., Devillers Ch. Bibliothéque de données nucléaires relatives aux produits de fission (4 éme édition): CEA-N-1822, 1975.
27.Mishra U.C. e.a. Fission and activation product data relevant to the studies on radioactive fallout from atmospheric nuclear explosions. India, Bombay, 1975.
28.Sola A. ISOTEX Code de calcul de concentrations isotopique et reports de concentrations. Euratom 1974.
29.Harte G.A. HYACINTH. A heavy isotope point burnup and decay code: RD/B/N 3564. Berkeley nucl. lab., 1976.
30.ANL 5800. Reactor physics constants. Sec.edition, 1963.
31. Gordeev I.V., Kardashev D.A., Malyshev V.A. Nuclear physics constants, Moscow (1963) (in Russian).
32. Elagin J.P. Resonance integrals of elements with Z = 90, Nuclear Constants, Moscow, 7, Atomizdat (1971) (in Russian).
33.Kunz W., Schintlmeister J. Tabellen der Atomkerne. Akademie Verlag Berlin, 1959.
34.Dillman L.T. Radionuclide decay schemes and nuclear parameters for use in radiation - dose estimation, nm/mird: Pamptlet ORNL, N 10.
35.Valenta V. New possibilities of calculating independent fission product yields: ZJE-207,1977.
36.Lammer, Eder. Discussion of fission products yields evaluation. Methods and a new evaluation: IAEA-SM-170/13, 1973.
37.Sidebotham. Fission product yields - data extrapolated for some actinides: TRG Rep. 2143 (R), 1972.
38.Abramowitz, Stegun. Handbook or mathematical functions National bureau of standards: AMS-55. Washington, 1966.
39. Gusev N.G. Radioactive characteristics of fission products, Moscow Atomizdat (1974) (in Russian).
40.Wahl e.a. Products from thermal neutron induced fission of ^{235}U a correlation of radiochemical charge and mass distribution data: IAEA-SM-127/116, 813.
41.Apalin e.a. Nucl.Phys., 1965, v.71, p.553.
42.Terrel. Neutron yields from fission fragments. - Phys.Rev., 1962, v.127, p.880-904.
43.Denschlag. Charge distribution in low energy fission reactors: IAEA-SM-122/126, 945.
44.Facchini. Energia Nucl., 1968, v.15, p.54.
45.Schwartzmann, Sieger, Yiftah. Conf. Geneva, 1964, P/511.
46. Pik Pičak, Strutinskij, Statistical fission theory, Nuclear Fission Physics, Moscow Atomizdat (1962) (in Russian).
47.Wahl. Physics and chemistry of fission: Proc.sympozium (Salzburg, 1965). V.I. IAEA, 1965, p.317.
48.Cuminghame, Goodall, Willis. Absolute yields in fission of ^{235}U, ^{238}U and ^{239}Pu irradiated in DFR: AERE-R6862 (rev.), 1972.
49.Wahl, Ferguson. Nuclear charge distribution in low-energy fission. - Phys.Rev., 1962, v.126, p.1112-1127.
50.Strom, Love. Phys.Rev., 1966, v.144, p.984.
51.Rhin e.a. IAEA-SM-122/150.
52.Amiel, Feldstein. Phys.Rev., 1975, v.C 3.
53.Bertram W.K. e.a. Group cross-section library: AAEC/E-214, 1971.

MEASUREMENT AND ANALYSIS OF NEUTRON SCATTERING CROSS-SECTIONS FOR THE NUCLEI OF STRUCTURAL MATERIALS IN THE 0.5-9.0 MeV REGION

I.A. Korzh

In view of the intensive development of nuclear power and the prospects for the utilization of fusion energy, a problem which is becoming increasingly important is that of supplying neutron data for nuclear power plant calculations, especially the differential and integral fast-neutron elastic and inelastic scattering cross-sections for the nuclei of iron, nickel and chromium (the main components of structural steels) and also those of molybdenum, zirconium, titanium and other elements used in refractory alloys and alloying additions. Moreover, there are prospects of using chromium, nickel and molybdenum in relatively high quantities (up to 40%) in fuel elements of dissociating-gas-cooled fast reactors.

Extensive data on fast-neutron scattering cross-sections for the nuclei of reactor and non-reactor material in wide ranges of mass numbers and neutron energies are also of theoretical importance in that they make it possible to verify the applicability of various nuclear models and to study the energy dependence of the scattering mechanism.

The practical needs of modern-day nuclear technology impose higher requirements as regards the accuracy and reliability of the experimental scattering cross-sections for the nuclei of structural materials. There is also a need for experimental neutron data on the cross-sections of all reactions. Such data do not exist in many cases, and the partial cross-sections obtained in various laboratories do not agree with each other. Experimental studies are not in a position for the time being to satisfy these needs fully. Solving the problem of supplying nuclear data for nuclear technology and for power plant calculations requires more than just new cross-section measurements: special importance is attached to new cross-section evaluations and to the improvement of the theoretical models

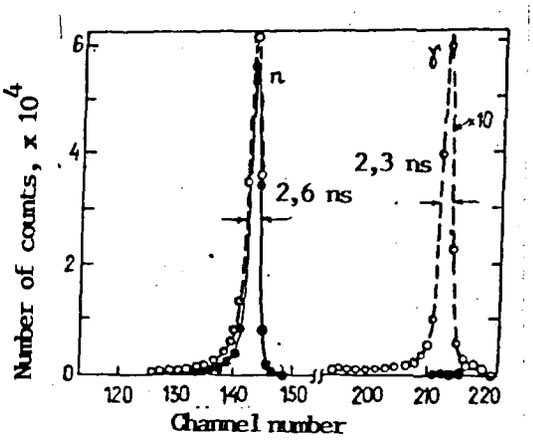

Fig. 1. Neutron spectra of the direct beam from the $T(p,n)^3He$ reactions with and without photon discrimination (continuous and broken lines, respectively): E_n = 3 MeV; $\theta = 0^o$; channel width 1.15 ns; path length 2.1 m.

which are used widely in calculations. It is on these questions that we focused in Refs [1-27].

The differential and integral neutron elastic and inelastic (with excitation of the first one-to-seven levels or groups of levels) scattering cross-sections were obtained for the ^{24}Mg, ^{48}Ti, ^{52}Cr, ^{54}Fe, $^{58,60,64}Ni$ and $^{92,94}Mo$ nuclei at 1.5, 2, 2.5, 3, 5, 6 and 7 MeV, for the ^{62}Ni, $^{76,78,80,82}Se$ and $^{126,130}Te$ nuclei at 1.5, 2, 2.5, 3 and 5 MeV, for the $^{50,54}Cr$, ^{56}Fe, $^{64,66,68}Zn$ and ^{209}Bi nuclei at 1.5, 2, 2.5 and 3 MeV and for the ^{16}O, ^{28}Si, ^{32}S and nickel nuclei at 5 MeV. These experimental data, together with the data of other authors at comparable energies, were analysed using the spherical optical model (OM), the statistical model and the coupled-channel (CC) model; for the sake of completeness, we also used the energy dependences of the total cross-sections and integral elastic and inelastic scattering cross-sections in the 0.5-9 MeV region. The data on the neutron elastic and inelastic scattering cross-sections for titanium, chromium, iron and nickel were compared with the results of present evaluations.

Experimental Procedure

The differential elastic and inelastic cross-sections with excitation of one-to-seven lowest levels (or groups of levels) for the nuclei under study were measured with the help of a time-of-flight spectrometer [1, 11] in a cylindrical geometry in the 20-150° range of angles. The parameters of the

fast-neutron time-of-flight spectrometer and the measurement conditions are given below:

Neutron sources	Reactions $T(p,n)^3He$ and $D(d,n)^3He$
Neutron energy	1-7 MeV
Targets (thickness 100-300 keV)	Titanium-tritium, scandium-tritium and titanium-deuterium on 0.1 mm thick molybdenum substrate
Distances:	
Target-sample	10 cm
Sample-detector	1.5-2.8 m
Neutron detector	5 x 5 cm stilbene crystal and photomultiplier FEhU-30
(n-γ) separation with photon suppression factor	10^3-10^4
Neutron recording threshold	Not less than 300 keV
Monitors	Time-of-flight spectrometer with 3 x 4 cm stilbene crystal and FEhU-30, "long counter" and current integrator
Spectrometer parameters:	
Non-linearity:	
Integral	0.3%
Differential	4.0%
Intrinsic time resolution	1.8 ns
Measurement angles	10-20 angles in the 20-150° range.

The spectra of scattered neutrons with initial energies of 1.5, 2, 2.5 and 3 MeV were measured using neutrons from the $T(p,n)^3He$ reaction. The total neutron energy spread due to finite target thickness, proton energy scatter and finite experimental geometry was 100-80 keV. The spectra of scattered neutrons with initial energies of 5, 6 and 7 MeV were measured with neutrons from the $D(d,n)^3He$ reaction, the total energy spread being 340-100 keV. It will be seen from Fig. 1 that the fast-neutron time-of-flight spectrometer has parameters comparable with the world's best spectrometers. These measurements were made on samples of high isotopic enrichment in the form of compacted powders of the isotopes (or their oxides) $^{58,60,62,64}Ni$, $^{64,66,68}Zn$, $^{50,52,54}Cr$, ^{54}Fe, $^{76,78,80,82}Se$, $^{92,94}Mo$ and $^{126,130}Te$ in thin-walled cylindrical containers. Part of the samples were of natural isotopic composition, but with the isotope under study predominating: ^{24}Mg, ^{28}Si, ^{32}S, ^{48}Ti, ^{56}Fe and ^{209}Bi. A hydrogen-containing material - polyethylene - was used as the reference material for the inelastic scattering cross-sections.

Measurement results

The differential elastic cross-sections were determined from the measured scattered neutron spectra by normalizing them to the neutron flux at zero angle and the differential inelastic cross-sections with excitation of one to seven levels for the isotopes under study were obtained by normalizing to the well-known scattering cross-section for hydrogen. For this purpose, apart from the spectra of neutrons scattered by the samples under study, measurements were also made of the spectra of the direct neutron beam and the spectra of neutrons scattered by the polyethylene sample. In the measurements on oxides, for determination of the elastic scattering cross-sections for the isotopes under study, those for oxygen were subtracted from the experimental elastic cross-sections for the corresponding oxides.

In the differential elastic and inelastic cross-sections corrections were made by the analytical method for attenuation of the neutron flux in the sample and for the anisotropy of neutron yield from the source; in the differential elastic cross-sections corrections were also made for the angular resolution of the experiment and for neutron multiple scattering in the sample [28].

The total errors of the measured cross-sections include statistical measurement errors (for elastic scattering up to 7% and at the minima up to 12%, for inelastic scattering up to 10% and at high energies for forward scattering angles up to 25%), errors in the scattering cross-sections for oxygen and hydrogen (1.5% for each) and errors associated with the cross-section calculation procedure. The presence of ^{16}O in oxide samples can lead to a 5-12% error, multiple scattering of neutrons has a 2-3% error, the anisotropy of neutron yield from the targets gives a 1.5% error, the neutron flux attenuation in the samples and in polyethylene leads to a 2% error in both cases, the angular resolution of the experiment contributes an error of up to 3% and the counting statistics of monitors up to 1%. The total measurement errors of the differential elastic cross-sections average 3-10%

for metallic samples and 6-15% for oxides; in the case of inelastic scattering, the average errors are 5-12% for all the isotopes studied at all angles except three forward scattering angles at high neutron energies, where the errors reach 16-25%. These satisfy current accuracy requirements for measurements of the differential elastic and inelastic cross-sections.

The total elastic and inelastic cross-sections were determined by integrating the differential cross-sections. As an example, the present study gives the experimental differential elastic and inelastic cross-sections in the 1.5-7 MeV region for the ^{48}Ti (Fig. 2), ^{52}Cr and ^{94}Mo (Fig. 3)[*] nuclei and also the data available from the literature [29-42] for comparable energies.

A characteristic feature of the measured angular distributions of elastically scattered neutrons in the energy region studied is the presence of a strong anisotropy manifested in the form of a sharp forward maximum, to which are added one or two more maxima in the cross-section in the 70-130° region of angles as neutron energy increases. During the study of differential elastic cross-sections for the even isotopes of nickel, selenium and molybdenum it was found that the shape of the angular distributions of cross-sections had an isotopic dependence, which indicated that the process was essentially optical in nature. In the 1-3 MeV region, for all the nuclei studied, the angular distributions of the inelastic cross-sections with excitation of individual levels or groups of levels are isotropic or symmetrical with respect to 90°, indicating the predominance of the inelastic scattering processes through the compound nucleus. At energies above 5 MeV an anisotropy in the form of an increase in cross-sections in the region of small scattering angles appears in the differential inelastic cross-sections with excitation of the first 2^+-levels of the nuclei studied: as the neutron energy increases, direct processes begin to play an increasingly important role in inelastic scattering.

---

[*] For ^{60}Ni a similar figure is given in Ref. [26], p. 62.

As an example of the measured energy dependences the present study gives the integral elastic and inelastic cross-sections for the natural titanium, ^{48}Ti (Figs 4 and 5), ^{52}Cr (Fig. 6) and ^{94}Mo (Fig. 7)[*] nuclei in the 1-7 MeV region; for purposes of comparison, these figures give the data of other authors, the results of present evaluations of those cross-sections and also the total interaction cross-sections in the 0.5-9 MeV region [29-36, 39-82]. The results of studies on elastic and inelastic scattering and the data on total cross-sections obtained with a high energy resolution which are presented here are averaged at intervals of 200 keV.

It can be seen from Figs 2 and 3 that, with some exceptions, the differential elastic and inelastic cross-sections obtained in different laboratories agree with each other. However, the integral cross-sections in Figs 4-7, representing the results of a much greater number of studies not reflected in the differential cross-sections in Figs 2 and 3, exhibit substantial spreads often exceeding experimental errors. This applies, principally, to the inelastic scattering data obtained from measurements of the associated photon yield and measurements on samples with natural isotopic composition.

An analysis of the literature on the fast-neutron scattering cross-sections for the nuclei studied revealed that most of the measured differential elastic and inelastic cross-sections had been obtained for the first time. Some of the experimental data obtained by the author significantly supplement and refine the existing data.

Theoretical analysis

New experimental data on scattering cross-sections, together with the data of other authors and those on total cross-sections, were analysed by the spherical optical model using the parameters obtained by the author and his co-workers and the optimal potential parameters available in the literature

---

[*] For ^{60}Ni a similar figure is given in Ref. [26], p. 65.

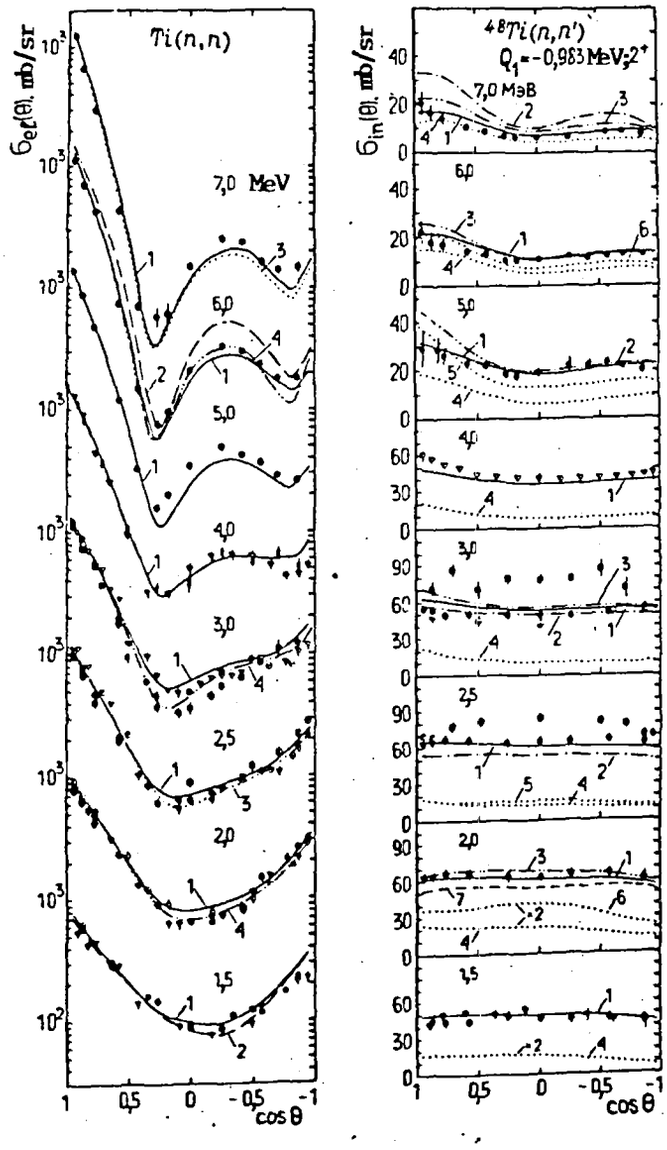

Fig. 2. Differential elastic and inelastic neutron scattering cross-sections in the 1.5-7.0 MeV region for the ^{48}Ti nucleus. Experimental data of: ● - authors [4, 27]; ▼- [29]; ▽ - [30]; ▮ - [31]; ⊖ - [32]; ◇ - [33]; ■ - [34]; ▭ - [35]; ⊖ - [36]. Calculations of elastic scattering cross-sections; curves 1,2 - by the spherical optical model (OM) and the Hauser-Feshbach-Moldauer model (HFM) with parameters (1) and those of Ref. [37]; curves 3,4 - by the coupled-channel (CC) method and HFM with parameters (1) and (2). Calculations of inelastic scattering cross-sections and components: curves 1-3 - by the CC model and HFM with parameters (1), those of Ref. [37] and (2); curves 4-6 - by the CC model with similar parameters; curve 7 - by HFM with parameters (1).

for the non-spherical optical model (coupled-channel method) and for the Hauser-Feshbach, Hauser-Feshbach-Moldauer and Tepel-Hofmann-Weidenmüller statistical models.

The theoretical analysis employing the optical-statistical approach was based on a set of averaged spherical potential parameters obtained by the author from a theoretical analysis of data on total cross-sections and polarized and non-polarized neutron elastic scattering cross-sections for nuclei with an average relative atomic mass in the 1.5-6.1 MeV region [83]:

$$V_c = (48.7 - 0.33E)\ \text{MeV}; \qquad a_v = a_{so} = 0.65\ \text{fm};$$
$$W_c = (7.2 + 0.66E)\ \text{MeV}; \qquad a_w = 0.98\ \text{fm}; \quad (1)$$
$$V_{so} = 7.5\ \text{MeV}; \qquad r_v = r_{so} = r_w = 1.25\ \text{fm}.$$

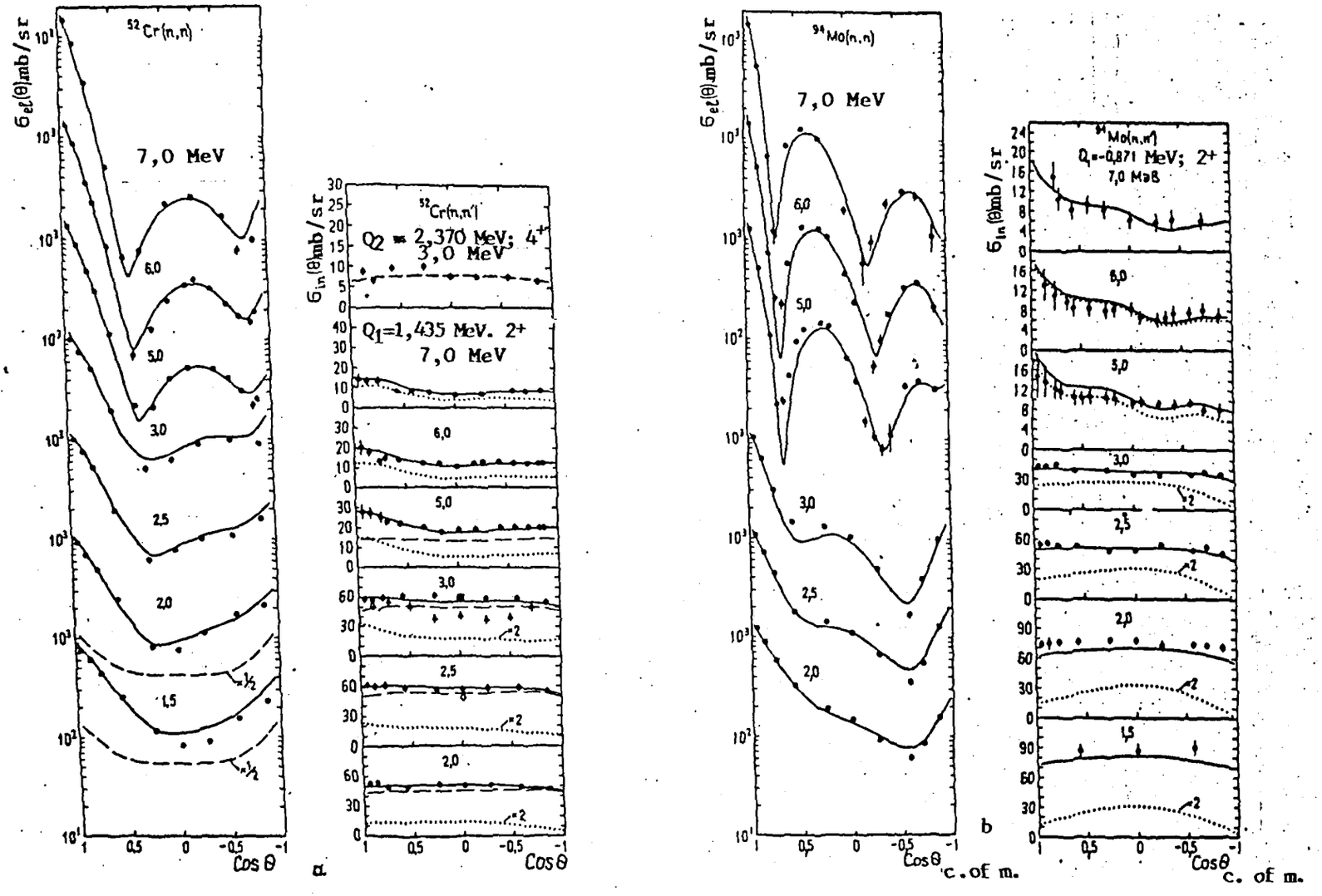

Fig. 3. Differential elastic and inelastic neutron scattering cross-sections in the 1.5–7.0 MeV region for the ^{52}Cr(a) and ^{94}Mo(b) nuclei. Calculations of cross-sections with parameters (1): continuous curves for elastic scattering – by the OM and HFM models, for inelastic scattering – by the CC and HFM models; dashed curves – by the HFM model; dotted curves – by the CC model. Experimental data for the ^{52}Cr nucleus: ● – authors [3, 5, 13, 16, 18, 20]; △ – [34]; ◇ – [35]; □ – [38]. For the ^{94}Mo nucleus the experimental data are from Refs [17, 19].

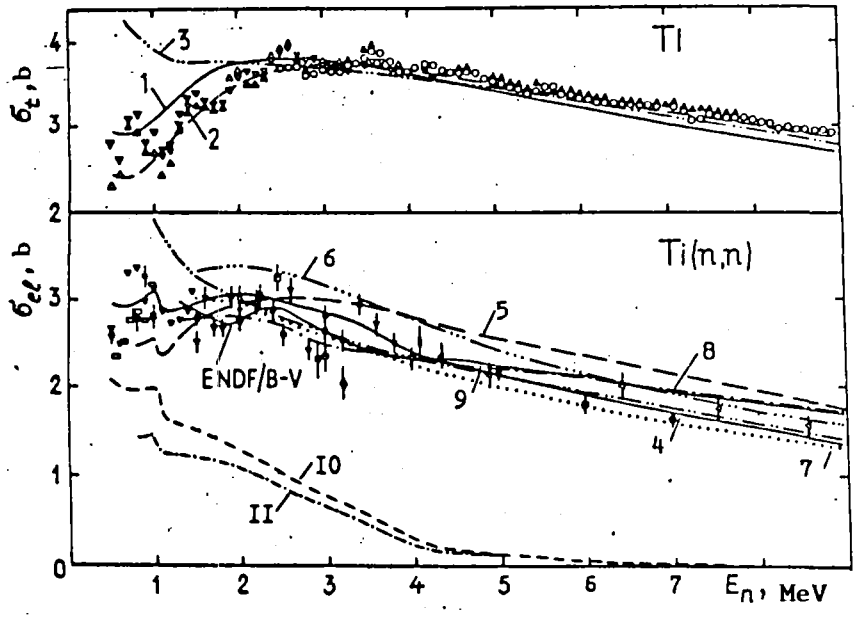

Fig. 4. Energy dependences of the total cross-sections and integral elastic scattering cross-sections for the titanium nucleus. Experimental data of: ● – authors [4, 27]; ▼ – [29]; ▽ – [30]; ■ – [31]; θ – [32]; ◇ – [33]; ■ – [34]; ◪ – [35]; ▭ – [43]; □ – [44]; ▨ – [45]; ◆ – [46]; ◁ – [47]; △ – [48]; 0 – [49]; ▲ – [50]. ENDF/B-V – evaluated cross-sections of Ref. [51] averaged at intervals of 200 keV. Calculations: curves 1–3 – total cross-sections by OM with parameters (1) and [37] and by the CC model with parameters (2); curves 4–6 – elastic scattering cross-sections by the OM and HFM models with parameters (1), [37] and (2); curves 7–9 – elastic scattering cross-sections by the CC and HFM models with parameters (1), [37] and (2); curves 10–11 – elastic scattering cross-sections by the HFM model with parameters (1) and [37].

In addition, the sets of optimal spherical optical potential parameters obtained from the analysis of total cross-sections for a wide range of energies [37] were used in the analysis of data for the titanium, chromium, iron and nickel nuclei.

Also used in the analysis was the set of averaged non-spherical optical potential parameters obtained for a wide range of energies and mass numbers [84]:

$$V_c = [51.85 - 0.33E - 24(N-Z)/A]\ \text{MeV}; \qquad r_o = 1.25\ \text{fm};$$
$$W_c = 2.55\sqrt{E}\ \text{MeV}; \qquad a_w = 0.48\ \text{fm}; \qquad (2)$$
$$V_{so} = 7.0\ \text{MeV}; \qquad a_v = a_{so} = 0.65\ \text{fm}.$$

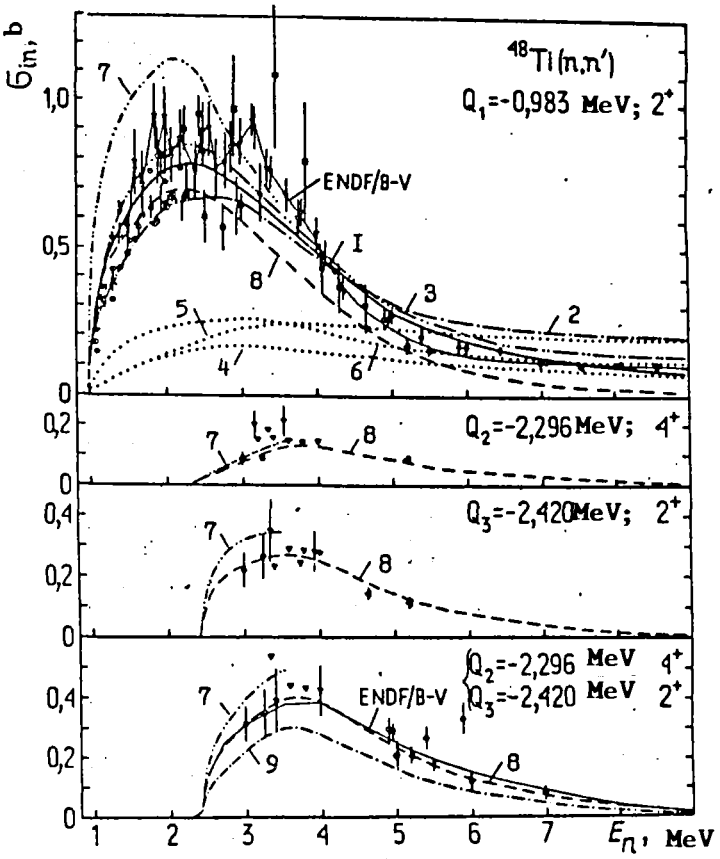

Fig. 5. Energy dependences of the integral inelastic neutron scattering cross-sections in the region from the threshold to 9.0 MeV with excitation of the three lowest levels for the ^{48}Ti nucleus. Experimental data of: ● - [2, 9, 27]; ▼ - [29]; ▽ - [30]; ■ - [34]; ◪ - [35]; ◍ - [36]; ◁ - [47]; ◪ - [52]; ◑ - [53]; ◐ - [54]; ◐ - [55]; X - [56]. ENDF/B-V - evaluated cross-sections of Ref. [51] averaged at intervals of 200 keV. Calculations: curves 1-3 - by the CC and HFM models with parameters (1), [37] and (2); curves 4-6 - by the CC model with parameters (1), [37] and (2); curves 7-8 - by the HF and HFM models with parameters (1); curve 9 - by the HFM model with parameters [37].

In the calculations of total cross-sections and direct elastic and inelastic scattering cross-sections using the coupled channel method [85] the interaction potential is presented in the form $V(r,\theta,\varphi) = V_{diag} + V_{coupl}$, where V_{diag} is the spherical optical potential and V_{coupl} its non-diagonal part leading to the coupling of reaction channels. In the coupled-channel method the problem reduces to selecting the coupling potential and calculating the matrix elements by a particular model for description of the structure of the lowest target-nucleus levels. In the case of spherical nuclei, generally

the vibration model with dynamic deformation is used. In this version of the coupled-channel model, the radius of the deformed components of the potential V_c and W_c is included in the form $R = R_o[1 + \Sigma_\mu \alpha_\mu Y2\mu(\theta,\varphi)]$, where $R_o = r_o A^{1/3}$ and $\langle O|\Sigma_\mu|\alpha\mu|^2|O\rangle = \beta_2^2$ (the parameter β_2 determines the coupling). Assuming that the lowest excited levels of nuclei are vibrational in nature, the author and his co-workers explicitly took into account only the coupling of the ground state with the first excitation ($0^+ - 2^+$). The coupled-channel calculations were performed using the complex coupling potential and the program described in Ref. [86]. The values of the coefficients of quadrupole deformation β_2 were taken from Refs [42, 87] and are given below:

^{28}Si 0,40	^{58}Ni 0,20	^{78}Se 0,27
^{32}S 0,37	^{60}Ni 0,22	^{80}Se 0,25
^{48}Ti 0,26	^{62}Ni 0,22	^{82}Se 0,22
^{50}Cr 0,30	^{64}Ni 0,20	^{92}Mo 0,II6
^{52}Cr 0,23	^{64}Zn 0,25	^{94}Mo 0,I69
^{54}Cr 0,27	^{66}Zn 0,22	^{126}Te 0,I63
^{54}Fe 0,I8	^{68}Zn 0,20	^{130}Te 0,I27
^{56}Fe 0,23	^{76}Se 0,28	

In the calculations by the spherical optical (OM) and coupled-channel (CC) models, for the same set of parameters, the value of the absorption potential varied in accordance with the relationship $W_c^{CC} = 0.8\ W_c^{OM}$, while the other parameters remained the same. This being so, the differences between cross-sections σ_t and σ_{el} calculated by the coupled channel and spherical optical models were small for all the nuclei studied, except those of the selenium isotopes [23].

The calculations of the compound elastic and inelastic cross-sections up to 3.5 MeV were performed by the statistical model without allowance for level width fluctuations (Hauser-Feshbach model [88]) and with allowance for these fluctuations (Hauser-Feshbach-Moldauer model [89]). At higher energies the compound cross-sections were calculated by both the Hauser-Feshbach-Moldauer model and the Tepel-Hofman-Weidenmüller model [90]. Up to 3.0-4.8 MeV the calculations by these variants of the statistical model took

account of discrete levels with known characteristics [91], while the contributions of the higher excited levels to the scattering cross-sections through the compound nucleus were taken into account as contributions of the continuum with a level density distribution determined by the Fermi-gas model with "back shift" with parameters a and Δ from Ref. [92].

The Hauser-Feshbach-Moldauer and Tepel-Hofmann-Weidenmüller formulae were obtained assuming independent reaction channels, i.e. in the case where the direct reaction cross-section is zero. In the presence of channel coupling the fluctuation cross-section can be calculated by the Hofmann-Richert-Tepel-Weidenmüller method [93]. Comparisons made of the compound cross-sections calculated by this method with those calculated by the Tepel-Hofmann-Weidenmüller method using transmission coefficients calculated by the coupled-channel method showed that the scattering cross-sections through the compound nucleus in the presence of channel coupling leading to the correlation of resonance widths does not differ much from the scattering cross-sections through the compound nucleus in the approximation of independent channels (the neutron inelastic scattering cross-sections for ^{60}Ni nuclei in the region up to 2.5 MeV calculated by the Hofmann-Richert-Tepel-Weidenmüller method are 5-7% higher than those calculated by the Tepel-Hofmann-Weidenmüller method).

In the statistical model calculations only the neutron emission channels were considered, while the competing channels with proton and alpha-particle emission were taken into account by the multiplier $(\sigma_c^{OM} - \sigma_{np} - \sigma_{n\alpha})/\sigma_c$, where σ_c^{OM} is the compound nucleus formation cross-section calculated by the spherical optical model. Since the statistical model calculations used transmission coefficients calculated by the spherical optical model, when the direct cross-sections were added to the compound cross-sections the latter were normalized by the multiplier $(\sigma_c^{OM} - \sigma_{2+}^{D})/\sigma_c^{OM}$, where σ_{2+}^{D} is the cross-section for direct excitation of the 2^+ level calculated by the coupled-channel method. Therefore, the total inelastic

cross-section with excitation of the first 2^+ levels of the nuclei studied is determined by the formula $\sigma^T_{nn'} = [(\sigma^{OM}_c - \sigma^D_{nn'})/\sigma^{OM}_c]\sigma^{CN}_{nn'} + \sigma^D_{nn'}$, where $\sigma^{CN}_{nn'}$ is the inelastic scattering cross-section through the compound nucleus. The validity of this formula is confirmed by the calculations of the total inelastic cross-sections using transmission coefficients calculated by the coupled-channel method.

The results of calculations by the above models are given in Figs 2-7 for the purpose of comparison with experimental data. The differential and integral elastic cross-sections are represented by sums of cross-sections calculated by the spherical optical or the coupled-channel model and by the Hauser-Feshbach-Moldauer statistical model.

In the 2-9 MeV region the calculated total cross-sections with the above-mentioned sets of parameters agree satisfactorily with the experimental data for all nuclei. At the beginning of the energy range under study, as was

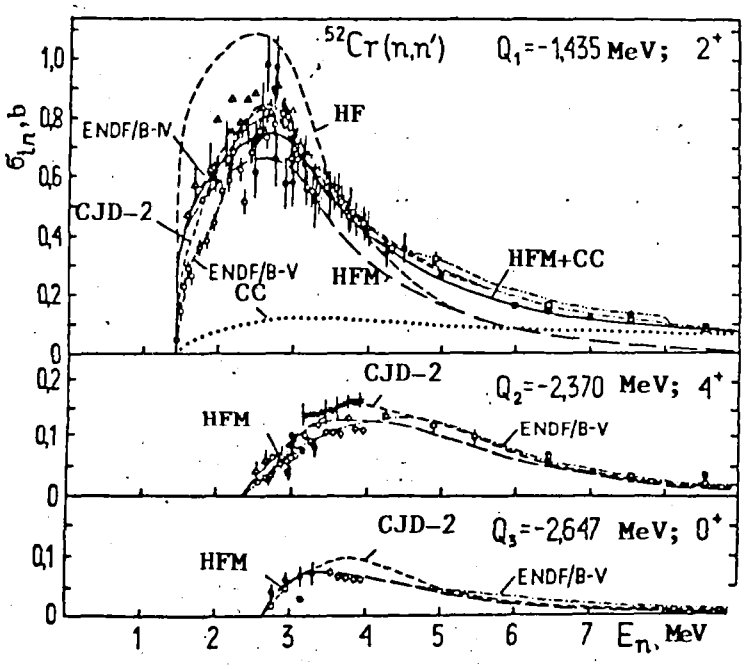

Fig. 6. Energy dependences of the neutron inelastic scattering cross-sections in the region from the threshold to 9.0 MeV with excitation of the three lowest levels for the ^{52}Cr nucleus. Experimental data of: ● - authors [2, 3, 5, 13, 16, 18, 20]; ■ - [57]; ○ - [58]; □,■ - [59]; ◐ - [60]; Δ - [61]; ◇ - [62]; ◍ - [63]. Curves - calculations by the different models with parameters (1) and also the data of the contemporary CJD-2 [64], ENDF/B-IV [65] and ENDF/B-V [66] evaluations.

to be expected, better agreement with experimental data is shown by the results of calculations with the set of optimal parameters from Ref. [37] and no agreement at all is shown by those with the set of non-spherical optical potential parameters (2). The total cross-sections calculated by the optical model with the parameters of Eq. (1) and of Ref. [37] do not differ much from one another (see Fig. 7). However, calculations with the set of parameters of Ref. [37] underestimate the contributions of the compound cross-sections to the total level-excitation cross-sections for the nuclei studied.

A comparison of the differential and integral elastic scattering cross-sections calculated by the spherical optical and coupled-channel methods with the experimental cross-sections indicated that in the region up to 3 MeV all sets of parameters [37, 83, 84] satisfactorily described the experimental data but that, as energy increased, calculations with the set of parameters from Ref. [37] showed significantly poorer agreement with experimental data.

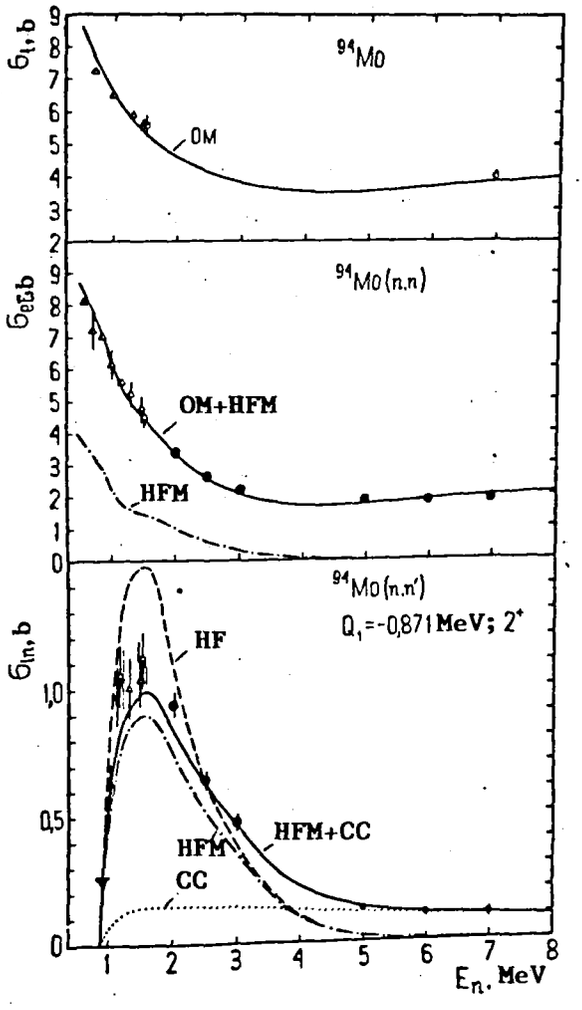

Fig. 7.

Energy dependences of the total elastic and inelastic scattering cross-sections with excitation of the three lowest levels for the ^{94}Mo nucleus. Experimental data of: ● - authors [17, 19]; ▼ - [56]; ◇ - [67]; △ - [68]; □ - [69]. Curves - calculation by the different models with parameters (1) (OM, HF, HFM and CC) and with the parameters of Ref. [37] (OM-1, HF-1, HFM-1, CC-1) and also data of the contemporary CJD-1 [70] and ENDF/B-IV [71] evaluations.

Cross-sections calculated by the spherical optical and coupled-channel methods exhibit minimal differences when the averaged parameters (1) are used; the use of the latter over the whole energy range results in satisfactory agreement with the experimental data on elastic scattering, fully reproducing the complication of the diffraction picture of scattering as energy increases.

In the energy range under study, calculations with the sets of parameters (1) and (2) give different contributions from both direct and compound scattering to the total cross-sections for excitation of the first 2^+-level for the nuclei studied. The total cross-sections also differ among themselves. The results of calculations with the set of parameters (1) agree better than others with experimental data as far as both the shape of angular distributions and the cross-section values are concerned. In the region from the excitation threshold to 3 MeV the total differential cross-sections calculated with the set of parameters (2) for nuclei with a high deformation parameter β_2 exhibit an anisotropy in angular distributions which was not observed in the experiments. As energy increases, calculations with sets of parameters (2) and [37] give an anisotropy in the angular distributions of cross-sections which differs increasingly from that observed experimentally. The integral cross-sections calculated with the set of parameters [37] are also substantially higher than the experimental cross-sections in the region above 5 MeV. Experiments show that, beginning already from the excitation threshold, even the cross-sections for direct excitation of the first 2^+-level make appreciable contributions to the total cross-sections and should therefore be taken into account.

In the energy range under study the excitation cross-sections for the second and subsequent levels are practically isotropic and are described quite satisfactorily by the statistical model, which indicates the dominant role played by the compound nucleus mechanism in the excitation of these levels. Calculations of the cross-sections for direct excitation of the two-phonon triplet levels for even isotopes of titanium, iron and nickel by the

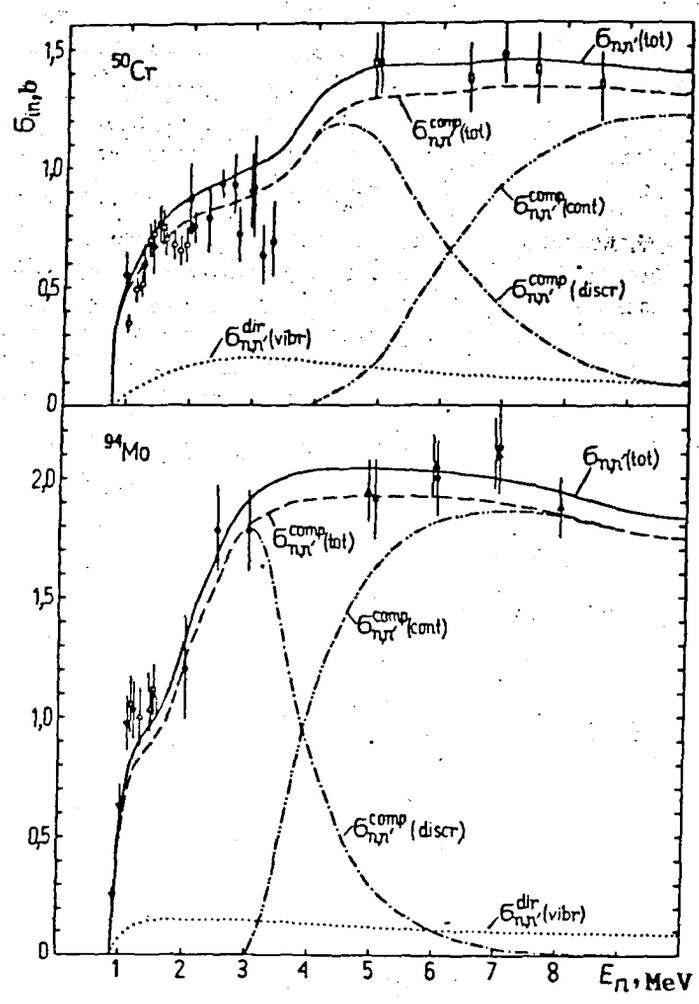

Fig. 8.

Energy dependences of the total inelastic neutron scattering cross-sections for the ^{50}Cr and ^{94}Mo nuclei. Experimental data for the ^{50}Cr nucleus: ●, ■ – authors [3, 16] (■ – for natural chromium); □ – [59]; ⊖ – [60]; ○ – [62]. Experimental data for ^{94}Mo: ● – authors [17, 19]; ▼ – [56]; Δ – [68]; ◻ – [69]; ▲ – [94] (for natural molybdenum). Curves – results of calculations by the statistical model and by the coupled-channel method.

five-channel variant of the coupled-channel method showed that these were approximately an order of magnitude smaller than the excitation cross-sections for the first 2^+-level.

Within the framework of the approach used, a satisfactory description was achieved also for the total inelastic cross-sections, obtained as the sum of the inelastic cross-sections with excitation of discrete levels or as the difference between σ_t and $(\sigma_{el} + \sigma_r)$; as an example, the results of calculation and experiment for the ^{50}Cr and ^{94}Mo nuclei in the region up to 10 MeV are compared in Fig. 8.

It will be seen from Fig. 8 that satisfactory agreement with experimental results is shown by the calculated cross-sections represented by the sum of direct inelastic scattering cross-sections $\sigma^{dir}_{nn'}(vibr)$ and scattering cross-sections through the compound nucleus $\sigma^{comp}_{nn'}(tot)$ $= \sigma^{comp}_{nn'}(discr) + \sigma^{comp}_{nn'}(cont)$, where $\sigma^{comp}_{nn'}(discr)$ is

the total inelastic scattering cross-section with excitation of discrete levels of known characteristics, and $\sigma_{nn'}^{comp}$(cont) is the inelastic scattering cross-section with excitation of higher levels of unknown characteristics.

Thus, the calculated total cross-sections and differential and integral elastic and inelastic cross-sections for nuclei with the average relative atomic mass in the 0.5-9.0 MeV region showed satisfactory agreement with the entire set of the author's experimental data and the data of other authors in calculations of scattering cross-sections through the compound nucleus using a statistical model which took into account level width fluctuations and with consideration of the direct excitation of the first 2^+-levels (beginning from the threshold).

The adequate theoretical description of the experimental data on neutron scattering obtained using the above approach made it possible to evaluate reliably the relative contributions of the scattering mechanisms (direct and compound) and their variation with incident neutron energy. Thus, the direct elastic scattering cross-section at the beginning of the energy range under study in these calculations is about 50% of the total cross-section, and at the end of the range it becomes predominant; at incident neutron energies of about 1 MeV above the excitation threshold of the first 2^+-level for the nuclei studied it does not exceed 15% of the total, and at the end of the energy range under study it becomes predominant. The large contribution of the direct mechanism to the excitation cross-sections for this level even at low incident neutron energies can be explained by the collective nature of the first excited states of the nuclei studied, because of which the probability of their direct excitation is increased by approximately an order in comparison with the excitation of single-particle levels.

The satisfactory theoretical description of a large number of experimental data for nuclei with an average relative atomic mass in a wide energy range (0.5-9.0 MeV) made possible a considerable reduction in the

uncertainty of the theoretical cross-sections due to the ambiguity of the theoretical model parameters. To sum up, the reliability of the theoretical cross-sections has reached such a level that the above procedure for the theoretical analysis of experimental data can be used to evaluate neutron cross-sections in those energy regions where there are contradictory experimental data or to predict them in energy regions where experimental data do not exist.

Comparison with evaluations

For titanium, chromium, iron and nickel isotopes, a comparison was made of the experimental cross-sections and the results of calculations with evaluated data obtained at the different centres (BNAB-78, Ts Ya D, ENDF/B-IV, ENDF/B-V, KEDAK-III and JENDL-I). This comparison is shown in Figs 4-7 for the energy dependences of the integral elastic and inelastic cross-sections for the nuclei of natural titanium, ^{48}Ti, ^{52}Cr and ^{94}Mo.

The results of the ENDF/B-V evaluation [51] of the elastic cross-sections for the natural titanium nuclei do not contradict the whole set of experimental data. For the chromium nuclei the best agreement with the set of experimental cross-sections is shown by the ENDF/B-V [66] and BNAB-78 [95] evaluations, while the evaluated cross-sections of the KEDAK-III [97] and JENDL-I system [96] differ noticeably from the experimental ones. Substantial differences are observed also between the evaluations of the average cosines of the elastic scattering angle, especially in the region below 2 MeV. This is due to the fact that some of the evaluations are based on different experimental studies. Of course, a more reliable evaluation can be obtained by taking into account the whole set of experimental data. It is precisely according to this principle that the evaluation of the average cosine of the elastic scattering angle was made for chromium (KIYaI[*]-83) [20]. The comparison in Ref. [26] of experimental data on integral fast-neutron elastic

---

[*] Translator's note: Kiev Institute for Nuclear Research.

scattering cross-sections for nickel nuclei with the ENDF/B-V evaluation results [98] averaged at intervals of 200 keV and with the data of the BNAB-78 group constant system [95] showed that in the region up to 4 MeV the ENDF/B-V evaluation results agreed satisfactorily with the experimental data, and that at energies above 4 MeV the evaluations were systematically higher than the experimental data by about 10%. There is excellent agreement of the data of the BNAB-78 group constant system and the experimental data obtained both before and after this system was set up.

For all the nuclei studied, the results of the different evaluations of inelastic cross-sections differ noticeably from each other, and sometimes there are appreciable differences between the evaluated data and the set of experimental data. As can be seen from Fig. 6, in the case of the inelastic cross-sections for ^{52}Cr in the 2 MeV region there are large differences between the evaluated data of the ENDF/B-IV and -V evaluations. For the first level of the ^{60}Ni nucleus at 2.0 MeV the ENDF/B-IV [71] and Ts Ya D-1 [70] evaluations differ by a factor of 1.5 [26]. Agreement with the experimental data on inelastic scattering cross-sections was also not improved by the ENDF/B-V evaluation [98] since the latter was based on one experimental study. Still greater differences exist between the KEDAK-III [97] and JENDL-I [99] evaluations and the experimental data on the inelastic cross-sections for ^{58,60}Ni nuclei. The considerable differences between the evaluation results reflect differences in approach and the complexity of the evaluation procedure itself. Greater confidence is inspired by the results of evaluations based on the set of available data on cross-sections.

The cross-sections measured by the author and the results of theoretical analysis made possible a more reliable evaluation of the neutron cross-sections for the nuclei of structural materials. These therefore formed the basis of the evaluation of the elastic and inelastic scattering cross-sections for chromium of natural isotopic composition and for chromium isotopes which was carried out in 1983 at the Nuclear Data Centre (Ts Ya D) of

the USSR State Committee on the Utilization of Atomic Energy [100] and recommended as the standard file to the national evaluated neutron cross-section library. In 1985 the Nuclear Data Centre made a new evaluation of the data for nickel and its isotopes, which was also based on our results for elastic and inelastic scattering cross-sections. At present, the evaluations which the Centre has performed in recent years best reflect the contemporary status of data.

REFERENCES

1. Zhuk, V.V., Kozar', A.A., Korzh, I.A., et al., in: Neutron Physics: Proceedings of the Second All-Union Conference on Neutron Physics, Kiev, 28 May-1 June 1973, Part 4, Obninsk (1974) 203 (in Russian).
2. Korzh, I.A., Kashuba, I.E., Golubova, A.A., in: Neutron Physics: Proceedings of the Third All-Union Conference on Neutron Physics, Kiev, 9-13 June 1975, Part 4, TsNIIatominform, Moscow (1976) 203 (in Russian).
3. Korzh, I.A., Mishchenko, V.A., Mozhzhukhin, Eh.N., et al., ibid. p.220
4. Korzh, I.A., Mishchenko, V.A., Mozhzhukhin, Eh.N., et al., Ukr. Fiz. Zh. 22 (1977) 87.
5. Korzh, I.A., Mishchenko, V.A., Mozhzhukhin, Eh.N., et al., Yad. Fiz. 26 (1977) 1151.
6. Korzh, I.A., Mishchenko, V.A., Mozhzhukhin, Eh.N., et al., Ukr. Fiz. Zh. 22 (1977) 112.
7. Korzh, I.A., Mishchenko, V.A., Mozhzhukhin, Eh.N., et al., Ukr. Fiz. Zh. 22 (1977) 866.
8. Korzh, I.A., Mishchenko, V.A., Mozhzhukhin, Eh.N., et al., Yad. Fiz. 26 (1977) 234.
9. Pravdivyj, N.M., Korzh, I.A., Mishchenko, V.A., et al., in: Neutron Physics: Proceedings of the Fourth All-Union Conference on Neutron Physics, Kiev, 18-22 April 1977, Part 1, TsNIIatominform, Moscow (1977) 273 (in Russian).
10. Korzh, I.A., Mishchenko, V.A., Pravdivyj, N.M., Izv. Akad. Nauk KazSSR, Ser. Fiz. Mat. 6 (1978) 61.
11. Korzh, I.A., Mishchenko, V.A., Sanzhur, I.A. Ukr. Fiz. Zh. 25 (1980) 109.
12. Korzh, I.A., Mishenko, V.A., Mozhzhukhin, Eh.N., et al., Yad. Fiz. 31 (1980) 13.
13. Pasechnik M.V., Korzh I.A., Mozhzhukhin E.N. In: Nucl. cross-sect. for technol.: Proc. of Intern. conf. (Knoxville,1979). Washington, 1980, p.893.
14. Korzh I.A., Mishchenko V.A., Mozhzhukhin E.N. e.a. Ibid., p.898.
15. Korzh, I.A., Lunev, V.P., Mishchenko, V.A., et al., in: Neutron Physics: Proceedings of the Fifth All-Union Conference on Neutron Physics, Kiev, 15-19 September 1980, Part 1, TsNIIatominform, Moscow (1980) 314 (in Russian); At. Ehnerg. 50 (1981) 398.
16. Korzh, I.A., Mishchenko, V.A., Mozhzhukhin, Eh.N., Pravdivyj, N.M., Yad. Fiz. 35 (1982) 1097.
17. Korzh, I.A., Mishchenko, V.A., Pravdivyj, N.M., in: Physics of Elementary Particles and Atomic Nuclei: Proceedings of the Conference on Nuclear Physics Research (Kharkov 1982), Part 2, TsNIIatominform, Moscow (1983) 144 (in Russian).
18. Korzh I.A., Mishchenko V.A., Pasechnik M.V., Pravdivy N.M. In: Nucl. data for sci. and technol.: Proc. of Intern. conf. (Antwerp, 1982). Holland, 1983, p.159.
19. Korzh, I.A., Lunev, V.P., Mishchenko, V.A., et al., in Problems of Atomic Science and Technology, Ser. Nuclear Constants No. 1(50) (1983) 40 (in Russian).
20. Korzh, I.A., Mishchenko, V.A., Pasechnik, M.V., Pravdivyj, N.M., in: Neutron Physics: Proceedings of the Sixth All-Union Conference on Neutron Physics, Kiev, 2-6 October 1983, Vol. 3, TsNIIatominform, Moscow (1984) 60 (in Russian).
21. Pravdivyj, N.M., Korzh, I.A., Lunev, V.P., Mishchenko, V.A., ibid. p. 78.
22. Korzh, I.A., ibid. p. 99.
23. Korzh, I.A., Mishchenko, V.A., Pravdivyj, N.M., ibid. p. 167.
24. Korzh, I.A., Lunev, V.P., Mishchenko, V.A., Pravdivyj, N.M., ibid. p. 173.
25. Korzh, I.A., Mishchenko, V.A., Pasechnik, M.V., Pravdivyj, N.M., At. Ehnerg. 58 (1985) 143.
26. Korzh, I.A., in: Problems of Atomic Science and Technology. Ser. Nuclear Constants No. 4 (1985) 61-71 (in Russian).
27. Korzh, I.A., Mishchenko, V.A., Pravdivyj, N.M., Yad. Fiz. 43 5 (1986) 1083-1091.

28. Engelbrecht C.A. Nucl. Instrum. and Methods, 1970, v.80, p.187; 1971, v.93, p.103; Block J., Jonker C. Physica, 1952, v.18, p.809.
29. Barnard E., de Villiers J., Reitmann D. e.a. Nucl. Phys., 1974, v.A229, p.189.
30. Smith A., Guenther P., Moldauer P., Whalen J. Ibid., 1978, v.A307, p.224.
31. Walt M., Beyster J. Phys. Rev., 1955, v.98, p.677.
32. Korzh, I.A., Mishchenko, V.A., Pravdivyj, N.M., et al., Ukr. Fiz. Zh. 11 (1966) 563; Korzh, I.A. I.A.,Mishchenko, V.A., Pasechnik, M.V., et al., Ukr. Fiz. Zh. 12 (1967) 1571; Pasechnik, M.V., Korzh, I.A., Kasgyba, I.E., et al., Yad. Fiz. 11 (1970) 958.
33. Kazakova L. Ya, Kolesov V.E., Popov V.I. e.a. In: Nucl. struct. study with neutrons: Proc. Intern. conf. Antwerpen, 1966, p.576.
34. Pasechnik, M.V., Fedorov, M.B., Yakovenko, T.I., in: Nuclear Physics Research in the USSR, No. 6, Atomizdat, Moscow (1986) 106 (in Russian).
35. Cranberg L., Levin J.S. Phys. Rev., 1956, v.103, p.343.
36. Etemad M.A. Aktiebolaget Atomenergi Rep. AE-481. Sweden: Studsvik, 1973.
37. Kawai M. Determination of spherical optical model parameters for structural materials. Contrib. to the topical discussion on "Progress in neutron cross-section measurements and evaluations concerning structural materials for fast reactors": NEANDC-Meeting. Belgium: Geel, 1979.
38. Gofman, Yu.V., Nemets, O.F., Tokarevskij, V.V., At. Ehnerg. 7 (1959) 477.
39. Boschung P., Lindow J.T., Shrader E.F. Nucl. Phys., 1971, v.A161, p.593.
40. Pasechnik, M.V., Fedorov, M.B., Yakovenko, T.I., in: Neutron Physics, Part I, Naukova Dumka, Kiev (1972) 277 (in Russian).
41. Smith A.B., Guenther P., Smith D., Whalen J. Nucl. Sci. and Engng, 1979, v.72, p.293.
42. Lachkar J., McEllistrem M.T., Haouat G. e.a. Phys. Rev., 1976, v.C14, p.933.
43. Langsdorf A., Jr., Lane R.O., Monahan J.E. Ibid., 1957, v.107, p.1077.
44. Lovchikova, G.N., At. Ehnerg. 12 (1962) 48.
45. Walt M., Barschall H. Phys.Rev., 1954, v.93, p.1062.
46. Becker R.L., Guindon W.G., Smith G.J. Nucl. Phys., 1966, v.89, p.154.
47. Kinney W.E., Perey F.G. Rep. ORNL-4810. Oak Ridge, 1973.
48. Cabe J., Cance M. Rep. CEA-R-4524. France, 1973.
49. Foster D.G., Jr., Glasgow D.M. Phys. Rev., 1971, v.C3, p.576.
50. Carlson A.D., Rothenberg L.M., Grimes S.M. Ibid., 1967, v.158, p.1142.
51. Philis C., Howerton R., Smith A. Titanium-II: An evaluated nuclear data file: ANL/NDM-28. Argonne, 1977.
52. Tsukada K., Tanaka S., Maruyama M. J.Phys.Soc. Japan, 1961, v.16, p.166.
53. Broder, D.L., et al., in: Nuclear Physics Research in the USSR, No. 2, Obninsk, (1966) 9 (in Russian)
54. Lashuk, A.I., Sadokhin, I.P., in: Nuclear Constants, No. 10, Atomizdat, Moscow (1972) 13 (in Russian)
55. Dickens J.K. Nucl. Sci. and Engng, 1974, v.54, p.191.
56. Konobeevskij, E.S., Musaelyan, R.M., Popov, V.I., et al., Fiz. Ehlem. Chastits At. Yadra 13 (1982) 300.
57. Smith A.B., Guenther P.T., Whalen J.F. In: Nucl. cross-section for technol.: Proc. Intern. conf. (Knoxville, 1979). Washington, 1980, N 594, p.168; Guenther P.T., Smith A.B., Whalen J.F. Nucl. Sci. and Engng, 1982, v.82, p.408.
58. Fedorov, M.B., Yakovenko, T.I., see Ref. [1], p. 56.
59. Kinney W.E., Perey F.G. Rep. ORNL-4806. Oak Ridge, 1974.
60. Van Patter D.M., Nath N., Shafroth S.M. e.a. Phys.Rev., 1962, v.128, p.1246.
61. Broder, D.L., Kolesov, V.E., Lashuk, I.P., et al., At. Ehnerg. 16 (1964) 103.
62. Karatzas P.T., Couchel G.P., Barnes B.K. e.a. Nucl. Sci. and Engng, 1978, v.67, p.37.
63. Almen-Ramstrom E. Aktiebolaget Atomenergi Rep. AE-503. Sweden: Studsvik, 1975.
64. Vozyakov, V.V., Bychkov, V.M., Lunev, V.P., Popov, V.I., in: Problems of Atomic Science and Technology. Ser. Nuclear Constants No. 4 (48) (1982) 44 (in Russian).
65. Prince A. Evaluation of chromium neutron and gamma-production cross-sections for ENDF/B-IV. N.Y.: Upton, 1976.
66. Prince A., Burrows T.W. Evaluation of nature chromium neutron cross-sections for ENDF/B-V. N.Y.: Upton, 1979.
67. Garber D.I., Kinsey R.R. (Eds.). Neutron cross-sections: BNL-325. 3rd ed. 1976, v.II.
68. Lambropoulos P., Guenther P., Smith A., Whalen J. Nucl. Phys., 1973, v.A201, p.1.
69. McDaniel F.D., Brandenberger J.D., Glasgow G.P., Leichton H.G. Phys. Rev., 1974, v.C10,p.108.

70. Bychkov, V.M., Popov, V.I., in: Problems of Atomic Science and Technology, Ser. Nuclear Constants No. 25 (1977) 55 (in Russian).
71. ENDF/B-IV, ^{28}Ni (MAT 1190). Evaluated by M.R.Bhat: BNL-17541, N.Y.: Upton, 1975.
72. Tsukada K., Tanaka S., Tomita Y., Maruyama M. Nucl. Phys., 1969, v.A125, p.641.
73. Perey F.G., Le Rigoleur C.O., Kinney W.E. ORNL-4523, UC-34-Physics, 1970; Kinney W.E., Perey F.G. ORNL-4807, 1974.
74. Towle J.H., Batchelor R., Gilboy W.B. In: Nucl. data for reactors: Proc. Intern. conf. (Paris, 1966). V.1. Vienna, 1967, p.367.
75. Rogers V.C., Beghian W.E., Clikeman F.M. Nucl. Sci. and Engng, 1971, v.45, p.297.
76. Towle J.H., Owens R.O. Nucl. Phys., 1967, v.A100, p.257.
77. Traiforos S., Mittler A., Schier W.A. e.a. Nucl. Sci. and Engng, 1979, v.72, p.191.
78. Fedorov, M.B., Ovdienko, V.D., Smetanin, G.A., Yakovenko, T.I., see Ref. [15] p. 309.
79. Konobeevskij, E.S., Kudenko, Yu. G., Popov, V.I., Skorkin, V.M., Yad. Fiz. 37 (1983) 1083.
80. Foster D.G., Jr., Glasgow D.W. Phys. Rev., 1971, v.C3, p.576.
81. Walt M., Becker R.L., Okazaki A., Fields R.E. Ibid., 1953, v.89, p.1271.
82. Musaelyan, R.M., Skorkin, V.M., in: Brief Communications in Physics No. 12 (1982) 28 (in Russian).
83. Pasechnik, M.V., Korzh, I.A., Kashuba, I.E., in: Neutron Physics, Part 1, Naukova Dumka, Kiev (1972) 253 (in Russian).
84. Tanaka S. JAERI-M 5984. Japan, 1975, p.212.
85. Tamura T. Rev. Mod. Phys., 1965, v.37, p.679.
86. Ignatyuk, A.V., Lunev, V.P., Shorin, V.S., in: Problems of Atomic Science and Technology. Ser. Nuclear Constants No. 13 (1974) 59 (in Russian).
87. Stelson P.H., Grodzins L. Nucl.Data, 1965, v.A1, p.21.
88. Hauser W., Feshbach H. Phys.Rev., 1952, v.87, p.366.
89. Moldauer P. Ibid., 1964, v.B135, p.642; Revs. Mod. Phys., 1964, v.36, p.1079.
90. Tepel J.W., Hofmann H.M., Weidenmuller H.A. Phys. Letters, 1974, v.B49, p.1.
91. Lederer C.M., Shirley V.S. (Eds.) Table of isotopes. 7th ed. N.Y., 1978.
92. Dilg W., Schantl W., Vonach H., Uhl M. Nucl. Phys., 1973, v.A217, p.269.
93. Hofmann H.M., Richert J., Tepel J.W., Weidenmuller H.A. Ann. of Phys., 1975, v.90, p.403.
94. Ловчикова Г.Н., Лунев В.П., Сальников О.А. и др. Ядерная физика, 1983, т.37, с.533.
95. Абагян Л.П., Базазянц Н.О., Николаев М.Н., Цыбуля А.М. Групповые константы для расчета реакторов и защиты. М.: Энергоиздат, 1981.
94. Lovichkova, G.N., Lunev, V.P., Sal'nikov, O.A., et al., Yad. Fiz. 37 (1983) 533.
95. Abagyan, L.P., Bazazyants, N.O., Nikolaev, M.N., Tsybulya, A.M., Group Constants for Reactor and Shielding Calculations, Ehnergoizdat, Moscow (1981) (in Russian).
98. Divadeenam M. Ni Elemental neutron induced reaction cross-section evaluation:BNL-NCS-51346 N.Y.: Upton, 1979.
99. Asami T., Tanaka S. Graphs of neutron cross-section data for fusion reactor development: JAERI-M-8136, 1979.
100. Belanova, T.S., Blokhin, A.I., Buleeva, N.N., et al., see Ref. [20] p. 54.